Science of the Total Environment 865 (2023) 161184

Contents lists available at ScienceDirect

Science of the Total Environment

journal homepage: www.elsevier.com/locate/scitotenv

Thermal stress gradient causes increasingly negative effects towards the range limit of an invasive mussel

Kevin C.K. Ma [a,b,*], Jonathan R. Monsinjon [a,c], P. William Froneman [a], Christopher D. McQuaid [a]

[a] Department of Zoology and Entomology, Rhodes University, Grahamstown, Eastern Cape, South Africa
[b] Department of Ocean Sciences, Memorial University of Newfoundland, St. John's, Newfoundland and Labrador, Canada
[c] Ifremer, Indian Ocean Delegation, Le Port, La Réunion, France

HIGHLIGHTS

- Gradient in thermal stress directly affected population dynamics towards species' range edge.
- Mussel abundance and recruitment increased with increasing distance from range edge.
- Disease-induced shell damage and epibiont load decreased with increasing distance from range edge.
- Shells of larger-sized mussels were more degraded and associated with more barnacle epibionts.

GRAPHICAL ABSTRACT

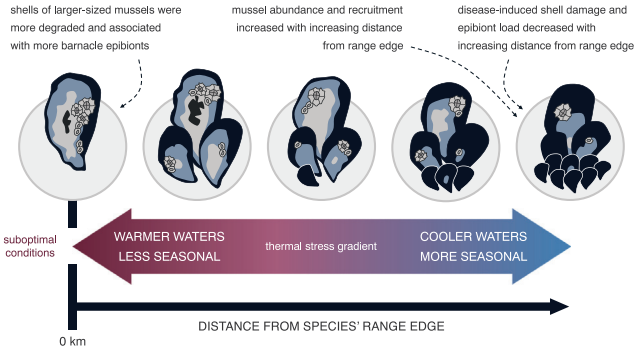

ARTICLE INFO

Editor: Julian Blasco

Keywords:
Basibiotic mussel
Effective shore level
Epibiotic barnacle
Mytilus galloprovincialis
Rocky shore
South Africa

ABSTRACT

Environmental filtering (EF), the abiotic exclusion of species, can have first order, direct effects with cascading consequences for population dynamics, especially at range edges where abiotic conditions are suboptimal. Abiotic stress gradients associated with EF may also drive indirect second order effects, including exacerbating the effects of competitors, disease, and parasites on marginal populations because of suboptimal physiological performance. We predicted a cascade of first and second order EF-associated effects on marginal populations of the invasive mussel *Mytilus galloprovincialis*, plus a third order effect of EF of increased epibiont load due to second order shell degradation by endoliths. Mussel populations on rocky shores were surveyed across 850 km of the south–southeast coast of South Africa, from the species' warm-edge range limit to sites in the centre of their distribution, to quantify second order (endolithic shell degradation) and third order (number of barnacle epibionts) EF-associated effects as a function of alongshore distance from the range edge. Inshore temperature data were interpolated from the literature. Using in situ temperature logger data, we calculated the effective shore level for several sites by determining the duration of immersion and emersion. Summer and winter inshore water temperatures were linked to distance from the mussel's warm range edge (our proxy for an EF-associated stress gradient), suggesting that seasonality in temperature contributes to first order effects. The gradient in thermal stress clearly affected densities, but its influence on mussel size, shell degradation, and epibiosis was weaker. Relationships among mussel size, shell degradation, and epibiosis were more robust. Larger, older mussels had more degraded shells and more epibionts, with endolithic damage facilitating epibiosis. EF associated with a gradient in thermal stress directly limits the distribution, abundance, and size structure of mussel populations, with important indirect second and third order effects of parasitic disease and epibiont load, respectively.

* Corresponding author at: Department of Zoology and Entomology, Rhodes University, Grahamstown, Eastern Cape, South Africa.
E-mail addresses: k.ma@ru.ac.za kevinckma@gmail.com (K.C.K. Ma).

http://dx.doi.org/10.1016/j.scitotenv.2022.161184
Received 5 July 2022; Received in revised form 16 December 2022; Accepted 21 December 2022
Available online 26 December 2022

1. Introduction

Environmental filtering (EF) is a mechanism by which the physical environment or habitat acts as a sieve for species with particular traits, which allows some species to become established and persist in a particular habitat while excluding others. This is likely to play a central role in explaining the incremental reduction in abundance as a species approaches its geographic range limits (Kraft et al., 2015; Valdivia et al., 2015). The effects of EF are often apparent at large spatial scales across biogeographic transition zones, where changes in species assemblages are pronounced (Sommer et al., 2014). Such transition zones are known to act as barriers to range shifts, altering the population dynamics of species at their range edges, an effect that can be exacerbated by climate change (Oldfather et al., 2020). For example, a geographic gradient of suboptimal abiotic conditions with accumulating negative effects on populations as they approach their range edges can reduce the growth, survival, and reproduction of individuals (Sagarin and Gaines, 2002; Paine et al., 2012). Despite being observable at larger spatial scales, such range edge dynamics can appear stochastic at finer spatial scales due to site-specific conditions (Anderegg and HilleRisLambers, 2019). In addition to the effects of EF in determining distributions and of EF-associated abiotic stress gradients in altering population structure (i.e., first order effects), variation in the effects of competitors, disease and parasites on host populations can be viewed as second order effects indirectly affected by EF. Changes to individual physiology and fitness, and to the population through changes in adult abundance or larval recruitment, due to such second order effects can lead to further consequences such as alterations to species interactions; these can be viewed as third order EF-associated effects. The cumulative outcome of this cascade of effects should theoretically be negative and can potentially explain EF-driven range edges.

Except for one species that is currently known to be undergoing rapid regional spread, i.e., *Semimytilus patagonicus* (Hanley, 1843) (see Ma et al., 2020), the distributions of intertidal marine mussels in South Africa are well-described and generally correspond to defined regions of biogeographic transitions in rocky shores (Zardi et al., 2007; Assis et al., 2015; Ma et al., 2021a). At the scale of bioregions, such patterns in South Africa can be explained by and are likely regulated by ocean current circulation patterns, which create distinctly different conditions of temperature and nutrient availability, and influence larval transport (Emanuel et al., 1992; Zardi et al., 2011; Assis et al., 2015). The major current systems characterising the South African coast profoundly influence coastal thermal regimes at large scales, helping to define the marine biogeography of South Africa's extensive coastline, including conditions that range from tropical to cool temperate. For mussels, species-specific thermal requirements help explain the absence of the native mussel *Perna perna* (Linnaeus, 1758) from cool temperate waters and the invasive mussel *Mytilus galloprovincialis* Lamarck, 1819 from warm subtropical waters (McQuaid et al., 2015; Tagliarolo and McQuaid, 2015). Nevertheless, biological interactions are also important. For example, both the invasive and native mussels exhibit infestation of the shell by photosynthetic cyanobacteria, which can cause shell degradation. Furthermore, the levels of endolithic infestation are higher in cooler bioregions than in warmer waters, i.e., cool temperate versus warm temperate, and warm temperate versus subtropical, respectively (Ndhlovu et al., 2019). In addition, mortality due to shell collapse caused by bioerosion induced by endolithic infestation is greater in the invasive mussel *M. galloprovincialis* than in the co-occurring native *P. perna*, probably because shells of the native species are generally thicker (Ndhlovu et al., 2019). Overall, these processes result in an inverse relationship between water temperature and level of endolithic infestation. Because of this, marine mussels are suitable target species to investigate range dynamics and the EF-associated effects of shell degradation induced by endolithic infestation of cyanobacteria (Zardi et al., 2009; Marquet et al., 2013; Ndhlovu et al., 2019) and barnacle epibiosis on shells (Bell et al., 2015) across large geographic distances.

Degradation of the shells of mussels and increased epibiosis load theoretically impart an energetic cost in terms of re-allocating resources from growth and reproduction towards improved attachment and shell repair (Henry and Hart, 2005). Physiological responses to endolithic infestation in mussels can include increased shell thickness, decreased mantle tissue, increase metabolic rates, and reduced fecundity, resulting in slower growth, and even mortality (Kaehler and McQuaid, 1999; Zardi et al., 2009; Gehman and Harley, 2019; Ndhlovu et al., 2021). On the other hand, endolithic microbes alter the colour and reflectance of infested shells, which may mitigate the warming effects of solar radiation, reduce body temperatures, and improve survival of infested mussels under heat stress compared to non-infested individuals (Zardi et al., 2016; Gehman and Harley, 2019; Monsinjon et al., 2021). Thus, the relationship between endolithic microbes and mussel hosts can be either mutualistic or parasitic, depending on environmental conditions (Gehman and Harley, 2019). At smaller spatial scales, endolithic colonisation of mussel shells is influenced by damage to the outer protective layer of the shell—the periostracum—and by the availability of light, which depends on height on the shore and the effects of small-scale shading (Kaehler, 1999; Zardi et al., 2009; Marquet et al., 2013; Gehman and Harley, 2019).

Endolithic infestation can also have indirect effects on host mussels by altering levels of epibiosis. Epibionts can interfere with feeding by filter feeders, alter predation pressure, and increase drag, requiring the host to redirect resources towards attachment (Buschbaum and Saier, 2001; Thieltges and Buschbaum, 2007a; Wahl, 2008). In the case of mussels, for example, barnacle epibionts can result in a suite of negative effects by slowing their rate of growth (Buschbaum and Saier, 2001) and increasing predation pressure from crabs (Enderlein et al., 2003). At the same time, the presence of barnacles on mussel shells can have a positive effect by reducing predation by sea stars (Laudien and Wahl, 1999, 2004). Barnacle recruitment tends to be greater on bare rock substratum (or rock mimic) than on live mussel shells, possibly because they avoid chemical antifouling cues from the periostracum (Scardino et al., 2003; Scardino and de Nys, 2004; Bers et al., 2006; Bell et al., 2015). Stable isotope and fatty acid analyses of free-living barnacles and mussels, epibiotic barnacles, and basibiotic mussels indicate an amensalistic relationship with the epibiont being negatively affected while the basibiont is unaffected (Puccinelli and McQuaid, 2021).

Three-species interactions, such as the relationships between endolithic infestation and host (second order EF-associated effects) and between barnacle epibiosis and host (third order effects), are likely a common phenomenon in nature. For example, similar dynamics have been documented in another multi-species interaction where the host, a marine snail is adversely affected by an endolithic polychaete worm, which in turn facilitates colonisation of barnacle epibionts on snails (Thieltges and Buschbaum, 2007b). Besides amensalistic interactions, symbiosis was reported in a three-way interaction among a marine mussel (the host), a parasitic micro-alga that promotes shell thickness, and shell-degrading endolithic cyanobacteria that facilitate survival of both the alga and the host by increasing light availability and mitigating against thermal stress, respectively (Zuykov et al., 2021). However, the outcomes of such complex dynamics and their response to abiotic stress gradients towards the host species' range edge remain largely unknown.

We investigated the effects of EF associated with a thermal stress gradient on the invasive mussel *M. galloprovincialis* along the south–southeastern coastline of South Africa. Specifically, we studied the interactions between shell degradation due to endolithic infestation and barnacle epibiosis across a thermal gradient from the host's range centre to its warm-edge range limit. To construct a composite inferential understanding of this multi-species interaction, we examined six specific relationships. First, mussel size (i.e., shell length) is expected to decrease towards the range edge because a gradient in thermal stress should substantially change the local population structure through increased mortality and decreased recruitment. Second, we expected that shell degradation (our proxy for endolithic infestation) will increase towards the warm range edge because exposure to suboptimal conditions could reduce the host's ability to produce quality periostracum. This should facilitate endolithic infestation, but the pattern would be reversed if solely regulated by climate (i.e., higher levels of endolithic infestation in cooler climates; Ndhlovu et al., 2019). Third, endolithic infestation was expected to increase with increasing mussel size because damage should accumulate as the host ages (e.g., Kaehler, 1999; Marquet et al., 2013). Fourth, we anticipated that barnacle epibiosis will increase towards to the host mussel's range edge for similar

reasons and, fifth, that the abundance of barnacle epibionts will be higher on shells of larger mussels because, sixth, barnacle abundance is expected to co-vary with endolithic infestation (e.g., Marquet et al., 2013).

2. Materials and methods

2.1. Collection of animals

Between 10 December 2019 and 16 November 2020, specimens of the focal host species, *Mytilus galloprovincialis*, were collected from 16 intertidal rocky shore sites in the species' South African range (Table A1 in the Appendix). These sites spanned ca. 850 km of coast from Tenza Beach in the east to Mosselbaai in the west (Fig. 1). Given the fractal characteristic of coastlines, this distance was determined by measuring the shore at 1-km intervals (see method in Ma et al., 2021b). At 10 sites (i.e., Tenza to Hamburg; Fig. 1) where abundances of *M. galloprovincialis* were below the likelihood of detection using quadrats, individuals were collected by hand by searching the entire height of the shore (predominantly the lower balanoid zone) and, if present, within patches of native mussels. At sites where *M. galloprovincialis* was more easily detected (i.e., six sites from Old Woman's River to Mosselbaai; Fig. 1), the populations were sampled using a 25 × 25 cm quadrat (n = 3 to 12 per site) placed haphazardly over the mussel bed. For each quadrat, dead mussels (e.g., empty shells) were separated from living individuals and discarded prior to determination of shell length (to the nearest 0.1 cm), estimation of shell degradation (our proxy for endolithic infestation), and enumeration of barnacle epibionts on shells.

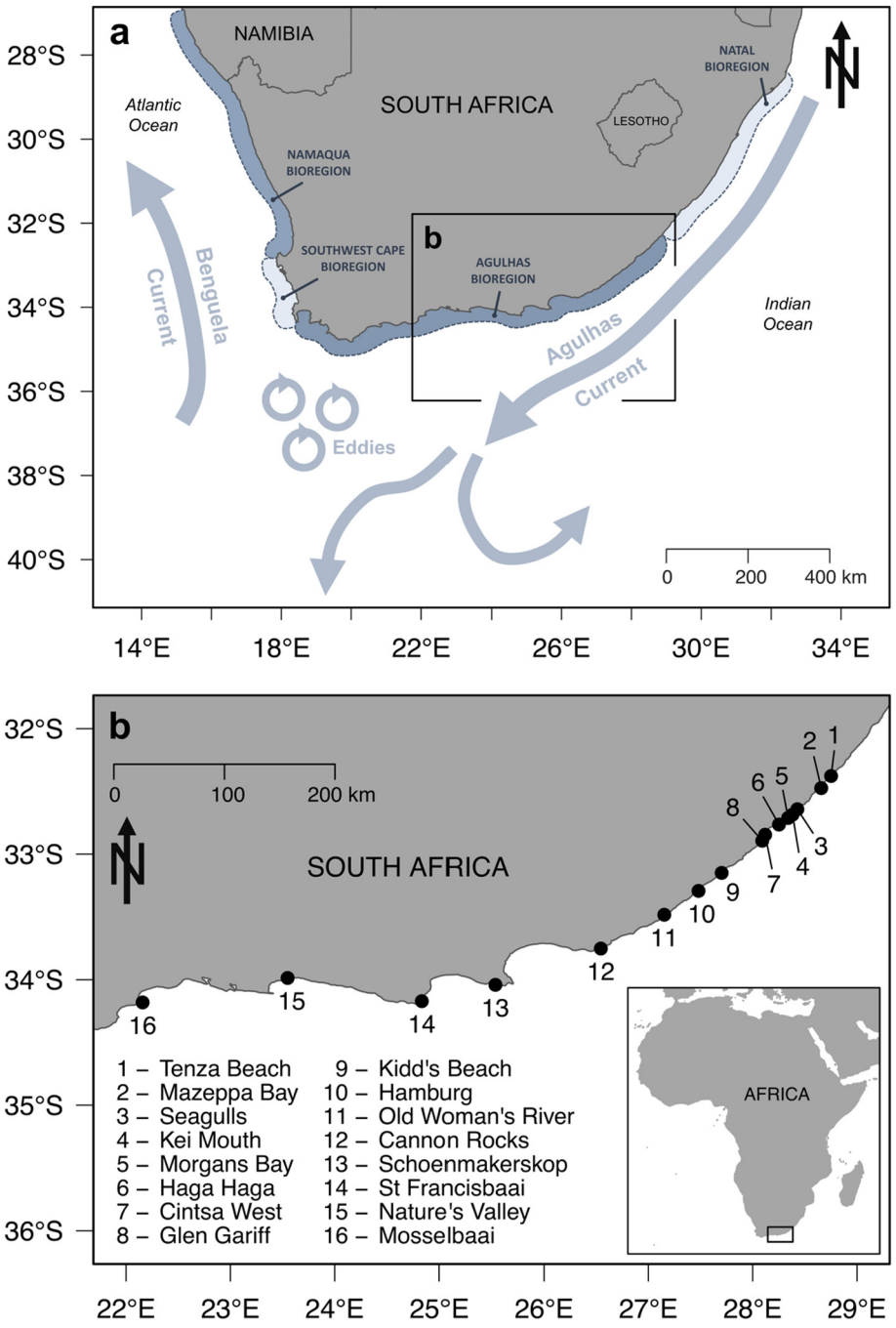

Fig. 1. Map of (a) marine bioregions and major coastal currents and (b) 16 sites where *Mytilus galloprovincialis* was sampled in South Africa.

2.2. Shell degradation

The percentage of the shell surface that exhibited endolithic degradation was estimated by eye as the mean of the two shell valves for each specimen of *M. galloprovincialis* and classified into one of six categories: 0 %, >0 to 25 %, >25 to 50 %, >50 to 75 %, >75 to <100 %, and 100 %. For analyses, we converted these categories into an index from 1 to 6 (i.e., from lowest to highest cover). This system differs from that used by others (e.g., Kaehler, 1999; Zardi et al., 2009; Marquet et al., 2013; Ndhlovu et al., 2019), which evaluates endolithic infestation by the degree of shell damage, because our hypothesis predicted that the number of barnacle epibionts would be proportional to the area of damaged shell rather than the degree of damage.

2.3. Barnacle epibionts on shells

Four species of barnacle epibionts were recorded on shells of live *M. galloprovincialis*: *Amphibalanus amphitrite* (Darwin, 1854), *Chthamalus dentatus* Krauss, 1848, *Octomeris angulosa* (Sowerby, 1825), and *Tetraclita serrata* Darwin, 1954 (Fig. A1 in the Appendix). The most common of these was *C. dentatus* (found on 21.3 % of mussels surveyed) and only this species was used in our analysis because abundances of the other three species were exceedingly low (each was found on <5 % of mussels). For our analyses, any *C. dentatus* that were growing on barnacle basibionts (i.e., not growing directly on the mussel shell) were not counted.

2.4. Abundances of barnacles and mussels on rocks

In-situ densities of free-living *C. dentatus* on emersed rocks (i.e., habitat exposed to air at low tide) in the mid balanoid zone (i.e., midlittoral zone; Stephenson and Stephenson, 1949) were determined from photographs made of twenty 50 × 50 cm quadrats placed at 0.5 m intervals along a 20-m transect line (i.e., one transect oriented parallel to the low tideline per site). Additionally, densities of *M. galloprovincialis* and the native mussel, *Perna perna*, in mono-layer mixed-species mussel patches were determined from photographs made of twenty 25 × 25 cm quadrats placed in the lower balanoid zone of the rocky shore (i.e., lower limit of the midlittoral zone; Stephenson and Stephenson, 1949). These quadrats were placed haphazardly on each shore to target mussel patches because these patches varied substantially in size and extent within (and among) sites. The lower size limit of mussels that were visible from the photo-quadrats was about 2 cm in length.

2.5. Relationship between length and planform area of shells

To estimate the density of barnacle epibionts on mussels (see Relationship #5b and related analyses below), the relationship between length and planform area was determined by measuring shell length and area of 25 mussel shells from each of five sites (i.e., Kidd's Beach, Old Woman's River, Cannon Rocks, Nature's Valley, and Mosselbaai; Fig. 1). These mussels were randomly selected from field collections (see above). For greater accuracy, the length of each specimen was measured to the nearest 0.001 cm. Specimens used for this analysis ranged from 0.674 to 5.208 cm in length. The planform area for each specimen was determined by dissecting the specimen and tracing the contour of one of its shells onto a gridded graph paper. The shell tracing was scanned in colour at a resolution of 600 dpi (dots per inch) as a digital image file and the Cartesian coordinates of the shell contour were extracted at every interval of 5 pixel in both the x and y coordinate axes from the scanned digital file using an online tool, *WebPlotDigitizer* (Version 4.4; Rohatgi, 2020). The coordinates were downloaded after sorting them by nearest neighbour to reconstruct a polygon shape, and the area of the reconstructed polygon was computed in the R programming environment (R Core Team, 2020). The relationship between shell length and area was determined by fitting a quadratic equation to the data with the intercept set at zero. This equation, i.e., $y = 0.2932x^2 + 0.3569x$ ($R^2 = 0.9862$; Fig. A2 in the Appendix), where x is shell length (centimetres) and y is planform area of one valve (squared centimetres), was used in subsequent analyses to estimate total shell area by multiplying by a factor of two to account for both valves of the mussels.

2.6. Temperature

Interpolated mean monthly inshore seawater temperature in February (austral summer) and August (austral winter) for sites where we collected animals and deployed temperature data loggers were estimated and extracted from the literature (Smit et al., 2013) using *WebPlotDigitizer*. Submersible temperature data loggers that recorded hourly (*EnvLogger* Version 2.4; precision of ≤0.1 °C and accuracy of ≤0.2 °C) were deployed on bare rocks that were emersed during low tide and in the vicinity of mussel beds for approximately 13 months from September 2019 to September 2020. These were

Table 1
Results of generalised linear models using the Gaussian error distribution and the identity link function; SE = standard error; statistically significant p values are in bold; df = degrees of freedom.

Dependent variable	Source	Estimate	SE	test statistic (t)	p
Mean monthly temperature in February (austral summer)	(intercept)	18.70000	0.27160	68.82	**<0.001**
	Distance from range edge	0.00298	0.00080	3.71	**0.002**
	Null deviance	16.9955 on 15 df			
	Residual deviance	8.5816 on 14 df			
	Deviance explained	0.50			
Mean monthly temperature in August (austral winter)	(intercept)	17.61205	0.10071	174.88	**<0.001**
	Distance from range edge	−0.00302	0.00030	−10.13	**<0.001**
	Null deviance	9.8295 on 15 df			
	Residual deviance	1.1796 on 14 df			
	Deviance explained	0.88			
In-situ densities of *C. dentatus* on emersed rocks	(intercept)	−174.45700	86.43500	−2.02	**0.044**
	Distance from range edge	3.40300	0.25600	13.29	**<0.001**
	Null deviance	614,041,932 on 319 df			
	Residual deviance	394,714,051 on 318 df			
	Deviance explained	0.36			
In-situ densities of *M. galloprovincialis* in mussel patches	(intercept)	−177.28450	58.65260	−3.02300	**0.003**
	Distance from range edge	2.87400	0.17370	16.54500	**<0.001**
	Null deviance	338,201,037 on 319 df			
	Residual deviance	181,750,253 on 318 df			
	Deviance explained	0.46			
In-situ densities of *P. perna* in mussel patches	(intercept)	317.82790	43.44940	−3.02300	**<0.001**
	Distance from range edge	0.45350	3.52400	16.54500	**<0.001**
	Null deviance	103,634,944 on 319 df			
	Residual deviance	99,739,856 on 318 df			
	Deviance explained	0.04			

placed at five sites: three sites within the study area in warm temperate waters (Old Woman's River, Nature's Valley, and Mosselbaai [$n = 3$ per site]) and two sites outside the study area in subtropical waters (Port Edward [$n = 1$] and Port Saint Johns [$n = 2$]; Fig. A3a in the Appendix). In-situ temperature values from data loggers were categorised into emersed and immersed conditions based on sudden drops in temperature during incoming tides to delineate the two conditions (Harley and Helmuth, 2003; Gilman et al., 2006; Helmuth et al., 2016). Using this method, the mean effective shore level (ESL; i.e., metres above mean lower low water [MLLW]) was determined for each site (i.e., logger data were pooled for a given site) using the timing of observed sudden drops and the predicted tidal level for the closest maritime port (Kampfer, 2017, 2018; Table A2 in the Appendix). When differences between emersed and immersed temperature at a given site were minute, sizable drops in temperatures were not observed, which, in the present study, was typical at our subtropical sites. As the accepted method was suitable for our three temperate sites but not for our two subtropical sites, we modified it by gradually increasing the temperature threshold (i.e., starting from $-16.5\ ^{\circ}C{\cdot}hr^{-1}$) until at least ten drops were detectable for each unique site (see our algorithm in Table A4 in the Appendix). Uncertain values from periods transitioning between the two conditions (e.g., due to the effects of strong wave action) were removed from the analysis. Instead of using a fixed buffer zone of 0.3 m around the mean ESL (e.g., Lathlean et al., 2011; Monaco et al., 2019), we re-defined uncertain values to comprise all values when tidal levels were greater than the mean ESL minus one standard deviation and less than the mean ESL plus one standard deviation for a given site (Table A2 in the Appendix). Local regression (LOESS) with a 15 % smoothing span was applied to the data to visualise overall seasonal trends. Using immersed temperature values, mean monthly temperatures in February 2020 and August 2020 were compared to the interpolated inshore temperature data extracted from Smit et al. (2013).

2.7. Characterisation of the thermal stress gradient

The warm-edge range limit was defined as beginning in Tenza Beach (i.e., distance of 0 km; Fig. 1) because extant populations are not known to occur east of this site in South Africa (Ma et al., 2021a). The alongshore distance of *M. galloprovincialis* populations from Tenza Beach served as our proxy for a gradient in thermal stress in all analyses. To characterise the overall patterns of the thermal gradient associated with EF, we evaluated the relationships between distance from range edge and five other variables. These were: (1) mean monthly temperature in February extracted from the literature, (2) mean monthly temperature in August extracted from the literature, (3) densities of *C. dentatus* (barnacles) on emersed rocks, (4) densities of *M. galloprovincialis* in mussel patches, and (5) densities of *P. perna* in mussel patches. These five relationships were assessed using generalised linear models (GzLMs) with the Gaussian error distribution and the identity link function. For these GzLMs and others performed in this study, several different error distributions (e.g., Gaussian, Poisson, Gamma) were tested and the error distribution associated with the lowest Akaike Information Criterion (AIC) value was selected as the model with the best fit for the data (Burnham and Anderson, 2002).

2.8. Effects of the thermal stress gradient

To evaluate the EF-associated effects of thermal stress, we examined the relationships between distance of host populations from the warm edge range limit at Tenza Beach (*Distance*) and the following three variables: mussel shell length (*Length*), percent cover of endolithic infestation (*Degradation*), and number of barnacle epibionts on shells (*Epibiosis*). We also examined the relationships between *Length* and *Degradation*, *Length* and *Epibiosis*, and *Degradation* and *Epibiosis*. None of the four variables (i.e., *Distance*, *Length*, *Degradation*, and *Epibiosis*) were normally distributed (Shapiro-Wilk normality test, W ranged from 0.233 to 0.988, $p < 0.001$ in all cases), even after data transformations. GzLMs were used to determine the relationship between each pair of variables.

The relationship between *Distance* (independent variable) and *Length* was assessed using a GzLM with a Gaussian distribution and an identity link function (Relationship #1a on all individuals). Due to potential site-specific variability in recruitment, we re-assessed this relationship by removing all settlers and recruits, defined as individuals that were <1.0 cm in length (Harris et al., 1998; Radloff et al., 2021), from the dataset (Relationship #1b on post-recruitment-sized individuals). We further investigated this relationship by considering only adults, defined as individuals that were >3.5 cm in length (Harris et al., 1998), in the GzLM (Relationship #1c on adult-sized individuals). Next, the relationships between *Distance* (independent variable) and *Degradation* (Relationship #2) and *Length* (independent variable) and *Degradation* (Relationship #3) were both examined using a GzLM with a Poisson distribution and a log link function. Because the distribution of barnacle (*C. dentatus*) epibionts on mussel shells consisted of zero-inflated values, two-component conditional models were used to evaluate relationships involving epibiosis. These were the relationships between *Distance* (independent variable) and *Epibiosis* (Relationship #4) and between *Degradation* (independent variable) and *Epibiosis* (Relationship #6). To compensate for the effects of mussel size, and thus shell surface area, the relationship between *Length* (independent

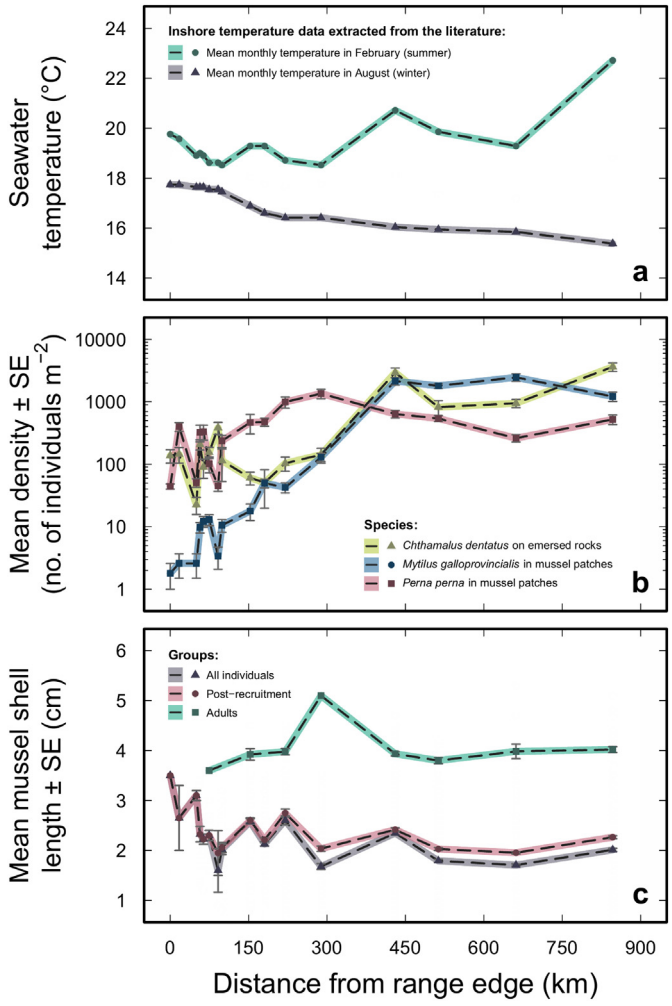

Fig. 2. Relationships between distance from warm-edge range limit of *Mytilus galloprovincialis* in South Africa and (a) seawater temperature ($N = 16$ data points), (b) densities of *Chthamalus dentatus* (barnacle) on emersed rocks ($N = 20$ data points per site), densities of *M. galloprovincialis* in mixed-species mussel patches ($N = 20$ data points per site), and densities of *P. perna* in mix-species mussel patches ($N = 20$ data points per site), and (c) mean shell length of *M. galloprovincialis* of all sized individuals, post-recruitment individuals (i.e., ≥1.0 cm), and adult-sized individuals (i.e., >3.5 cm); temperature data were extracted from Smit et al. (2013); y-axis of panel 'b' is log scale.

variable) and *Epibiosis* was separately based on epibionts abundance (Relationship #5a) and epibionts density (Relationship #5b; see relationship between length and planform area described above). For the first component of the conditional model, GzLMs with a binomial distribution and a logit link function were applied to presence/absence data. For the second component of the conditional model, GzLMs with a Poisson distribution and a log link function were applied on a zero-truncated dataset. Because there are nine ecological comparisons on the same data (i.e., Relationships #1a, #1b, #1c, #2, #3, #4, #5a, #5b, and #6), a Bonferroni correction of the alpha level of 0.05 divided by nine was applied.

To further examine Relationship #2, i.e., the relationship between *Distance* and *Degradation*, the data were partitioned into five size-classes of mussel shell lengths: ≤1.0, >1.0 to 2.0, >2.0 to 3.0, >3.0 to 4.0, and >4.0 cm. A partitioned GzLM using a Poisson distribution and a log link function was performed on the dataset for each of the five size-classes.

Similarly, the data were partitioned into four size classes of shell lengths: >1.0 to 2.0, >2.0 to 3.0, >3.0 to 4.0, and >4.0 cm to further investigate Relationships #4 and #6, i.e., the relationships between *Distance* and *Epibiosis* and between *Degradation* and *Epibiosis*. Because no barnacle epibionts were found on the smallest size-class of shell lengths (≤1.0 cm), data belonging to this size-class was not used in the partitioned analyses. A two-component conditional model was applied on each of the four size-classes. The first and second components of the partitioned conditional models consisted of a GzLM with a binomial distribution and a logit link function on presence and absence data and a GzLM with a Poisson distribution and a log link function on zero-truncated data, respectively. All graphical visualisations and statistical analyses were computed using the R programming environment (R Core Team, 2020).

3. Results

3.1. Characterisation of the thermal stress gradient

3.1.1. Interpolated temperatures from the literature

Unexpectedly, sites that were farther from the eastern warm-edge range limits of *Mytilus galloprovincialis* generally exhibited warmer mean water temperatures in summer than western centre-of-range sites. In austral summer (February), temperatures ranged from 22.7 °C at center sites in the west to 19.2 °C at range edge sites in the east. In contrast, winter (August), temperatures were cooler at center sites in the west (15.4 °C) than at range edge sites in the east (17.7 °C). This resulted in more pronounced seasonal differences between summer and winter temperatures as a function of *Distance* (Table 1 and Fig. 2a). Furthermore, *Distance* explained 88 % of the variation (i.e., deviance explained) in mean monthly summer temperatures and 50 % of the variation in mean monthly winter temperatures (Table 1).

3.1.2. In-situ temperatures from data loggers

During winter, (August) mean sea temperatures increased from 16.2 °C at warm temperate centre sites in the west (i.e., the region where EF does not exclude *M. galloprovincialis*) to 20.2 °C at subtropical sites outside the host species' range in the east (i.e., region where EF excludes the species; Fig. A3a, b in the Appendix). During summer (February), temperatures within the warm temperate range of *M. galloprovincialis* decreased from a mean of 16.2 °C in the west to 20.9 °C in the east. Temperatures did, however, increase at the subtropical sites farther east of the range edge, to 22.9 °C at Port Saint Johns and 24.5 °C at Port Edward (Fig. A3b,c in the Appendix). Although there were some differences in mean monthly values (Fig. A3c in the Appendix), seasonal patterns across the five sites were similar for historical, interpolated values from the literature and recent values recorded by our data loggers. In particular, mean monthly values differed by as little as <0.1 °C and as much as 2.1 °C during summer in February (average difference of 1.2 ± 0.9 °C) and by as little as 0.6 °C and as much as 1.1 °C during the winter in August (average of 0.9 ± 0.2 °C; Fig. A3c in the Appendix). Moreover, only two interpolated temperatures from the literature were outliers (e.g., one datum from Port Edward in February and one from Port Saint Johns in August) when compared with in-situ immersed temperatures recorded by our temperature loggers (Fig. 3). Thermal differences between emersed and immersed conditions were most pronounced during the summer from sites in warm temperate waters (i.e., sites within our study area) but not from sites in subtropical waters (i.e., sites outside our study area; Fig. A4 in the Appendix).

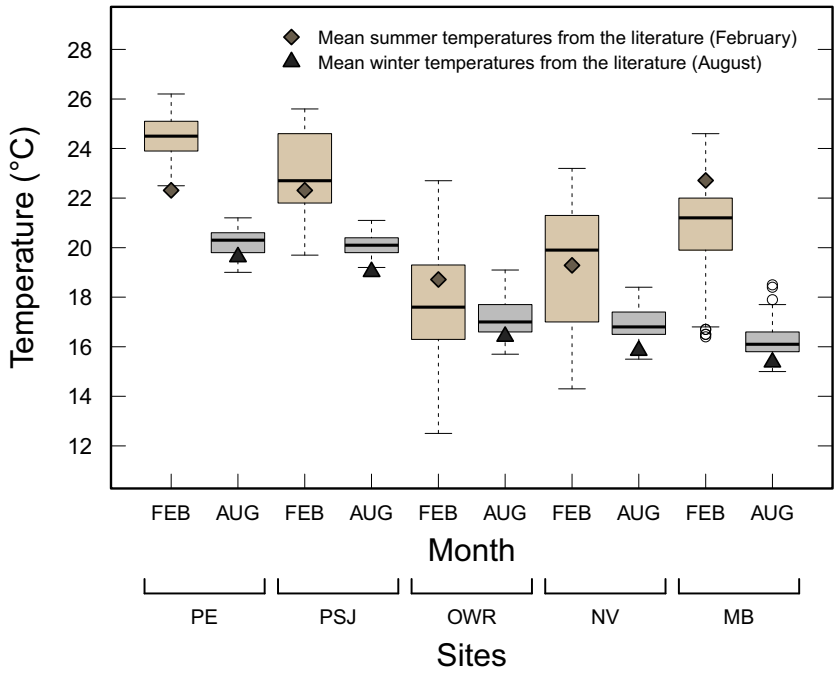

Fig. 3. Immersed temperatures in February 2020 (austral summer) and August 2020 (austral winter) from each of the five sites and mean monthly interpolated inshore temperature data extracted from the literature, i.e., Smit et al. (2013), for the corresponding months of February and August; PE = Port Edward (subtropical waters); PSJ = Port Saint Johns (subtropical waters); OWR = Old Woman's River (warm temperate waters); NV = Nature's Valley (warm temperate waters); MB = Mosselbaai (warm temperate waters).

3.1.3. Abundances of barnacles and mussels on rocks

In-situ densities of barnacles, *Chthamalus dentatus*, on emersed rocks and mussels, *M. galloprovincialis*, in mussel patches tended to increase with increasing distance from the range edge of *M. galloprovincialis*. Distance explained about 36 and 46 % respectively of this variation (Table 1 and Fig. 2b). Although this distance was also a significant predictor of in-situ densities of *Perna perna* in mussel patches, it explained only 4 % of the spatial variation in *P. perna* density. Across the 16 sites, mean densities of *C. dentatus* ranged from 22 individuals m^{-2} at Seagulls to 3,630 individuals m^{-2} in Mosselbaai. Numbers of *M. galloprovincialis* ranged from <1 individuals m^{-2} at Tenza Beach to 2467 individuals m^{-2} at Nature's Valley, and numbers of *P. perna* from 43 individuals m^{-2} at Tenza Beach to 1356 individuals m^{-2} at Cannon Rocks (Figs. 1 and 2b).

3.2. Effective shore levels

Using our modified method, ESL values ranged from 0.943 to 1.260 m among the five rocky shore sites where we had data loggers (Table A2 in

Table 2
Results of generalised linear models (Relationships #1a, #1b, #1c, #2, and #3) and two-component conditional models (#4, #5a, #5b, and #6); SE = standard error; statistically significant *p* values are in bold and have been adjusted using the Bonferroni correction to the alpha level of 0.0056 because there are nine ecological comparisons on the same data; df = degrees of freedom.

Relationship (component)	Dependent variable	Error distribution	Source	Estimate	SE	test statistic (*t* or *z*)	*p*
#1a	Shell length (all sized individuals)	Gaussian	(intercept)	2.26902	0.03434	66.07	**<0.001**
			Distance from range edge	−0.00054	0.00005	−9.36	**<0.001**
			Null deviance	3,091.4 on 4,110 df			
			Residual deviance	3,026.9 on 4,109 df			
			Deviance explained	0.02			
#1b	Shell length ≥1.0 cm (post-recruitment)	Gaussian	(intercept)	2.36000	0.03069	76.90	**<0.001**
			Distance from range edge	−0.00033	0.00005	−6.18	**<0.001**
			Null deviance	1920.1 on 3,536 df			
			Residual deviance	1,899.6 on 3,535 df			
			Deviance explained	0.01			
#1c	Shell length >3.5 cm (adults)	Gaussian	(intercept)	3.91157	0.06771	57.77	**<0.001**
			Distance from range edge	0.00010	0.00012	0.86	0.394
			Null deviance	18.32 on 145 df			
			Residual deviance	18.23 on 144 df			
			Deviance explained	<0.01			
#2	Shell degradation	Poisson	(intercept)	1.47094	0.02030	72.44	**<0.001**
			Distance from range edge	−0.00037	0.00004	−10.50	**<0.001**
			Null deviance	3,837.3 on 4,110 df			
			Residual deviance	3,727.9 on 4,109 df			
			Deviance explained	0.03			
#3	Shell degradation	Poisson	(intercept)	0.48768	0.02246	21.71	**<0.001**
			Shell length	0.37092	0.00924	40.15	**<0.001**
			Null deviance	3,837.3 on 4,110 df			
			Residual deviance	2,253.3 on 4,109 df			
			Deviance explained	0.41			
#4 (first)	Presence and absence of epibionts on shells	Binomial	(intercept)	−2.32628	0.12186	−19.09	**<0.001**
			Distance from range edge	0.00115	0.00019	5.92	**<0.001**
			Null deviance	3,585.8 on 4,110 df			
			Residual deviance	3,549.3 on 4,109 df			
			Deviance explained	0.01			
#4 (second)	Zero-truncated abundance of epibionts on shells	Poisson	(intercept)	1.81545	0.04944	36.72	**<0.001**
			Distance from range edge	−0.00043	−0.00008	−5.37	**<0.001**
			Null deviance	4,098.1 on 648 df			
			Residual deviance	4,069.6 on 647 df			
			Deviance explained	<0.01			
#5a,b (first)	Presence and absence of epibionts on shells	Binomial	(intercept)	−4.83540	0.16670	−29.00	**<0.001**
			Shell length	1.38410	0.06350	21.80	**<0.001**
			Null deviance	3,585.8 on 4,110 df			
			Residual deviance	2,953.9 on 4,109 df			
			Deviance explained	0.18			
#5a (second)	Zero-truncated abundance of epibionts on shells	Poisson	(intercept)	−0.68851	0.08293	−8.30	**<0.001**
			Shell length	0.77502	0.02630	29.47	**<0.001**
			Null deviance	4,098.1 on 648 df			
			Residual deviance	3,270.1 on 647 df			
			Deviance explained	0.20			
#5b (second)	Zero-truncated estimated densities of epibionts on shells (to compensate for surface area of shells)	Poisson	(intercept)	−1.01025	0.21225	−4.76	**<0.001**
			Shell length	0.22617	0.07298	3.10	**0.002**
			Null deviance	458.4 on 648 df			
			Residual deviance	448.9 on 647 df			
			Deviance explained	0.02			
#6 (first)	Presence and absence of epibionts on shells	Binomial	(intercept)	−4.53930	0.18536	−24.49	**<0.001**
			Shell degradation	0.68784	0.03876	17.75	**<0.001**
			Null deviance	3,585.8 on 4,110 df			
			Residual deviance	3,120.6 on 4,109 df			
			Deviance explained	0.13			
#6 (second)	Zero-truncated abundance of epibionts on shells	Poisson	(intercept)	−0.74613	0.11619	−6.42	**<0.001**
			Shell degradation	0.46148	0.02213	20.85	**<0.001**
			Null deviance	4,098.1 on 648 df			
			Residual deviance	3,576.0 on 647 df			
			Deviance explained	0.13			

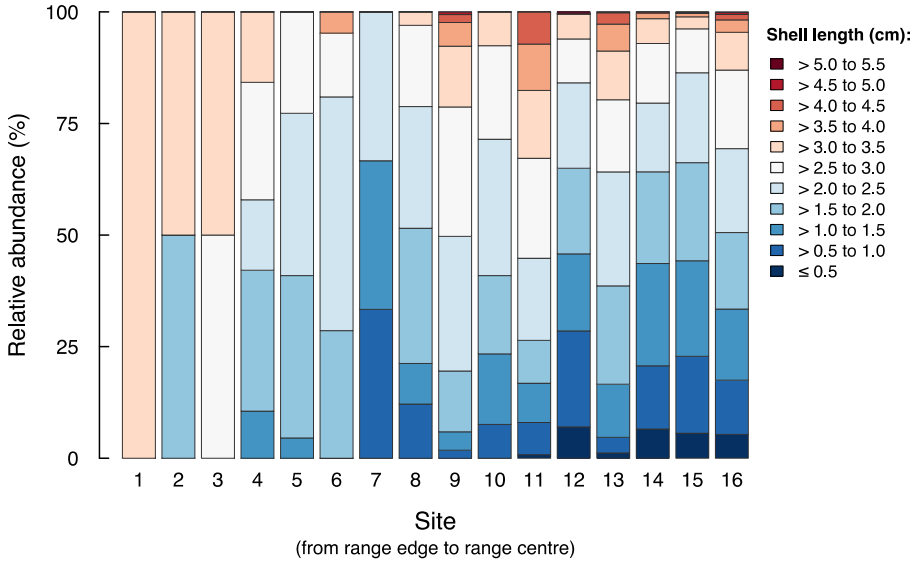

Fig. 4. Relative abundance of different shell lengths of *Mytilus galloprovincialis* in South Africa from range edge to range centre sites; see Table A1 in the Appendix and Fig. 1 for the name and location of the numbered sites.

the Appendix). The conventionally-accepted threshold of -16.5 °C·hr^{-1} used to detect sudden drops in temperature (i.e., roughly corresponding to those thresholds recommended by Gilman et al., 2006 for application in temperate systems) was suitable for two intertidal sites located in warm temperate waters (Old Woman's River and Nature's Valley). However, higher temperature thresholds (> -16.5 °C·hr^{-1}) for the other three sites—one in warm temperate waters (Mosselbaai) and two in subtropical waters (Port Edward and Port Saint Johns)—were required to produce at least ten drops (Table A2 in the Appendix). No sudden drops were detected for either of our subtropical sites when the conventionally-accepted threshold was used, necessitating the implementation of substantially higher thresholds for the subtropical sites of Port Edward and Port Saint Johns (-3.9 and -9.7 °C·hr^{-1}, respectively) than for our three warm temperate sites.

3.3. Relationship # 1: distance from range edge and shell length

When all post-recruitment individuals (≥1.0 cm in shell length) were considered in the analyses, shell lengths in mussel populations (*Length*) weakly decreased with increasing distance from the warm-edge range limit (*Distance*; Table 2 and Fig. 2c). However, no relationship between *Length* and *Distance* was found for adult-sized individuals (>3.5 cm; Table 2 and Fig. 2c). Compared to those at the range edge, populations at centre sites tended to have greater variation in shell lengths, consisting of both small, immature individuals (i.e., settlers and recruits) and adults (Fig. 4). Despite being a significant predictor of *Length*, *Distance* explained only about 2 % of total variation when all individuals were considered, and 1 % for post-recruitment individuals only (Table 2).

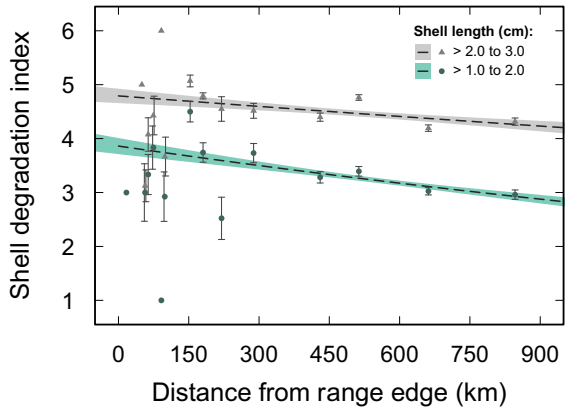

Fig. 5. Relationship between distance from warm-edge range limit in South Africa and mean (± SE) shell degradation index value in two intermediate size-classes of *Mytilus galloprovincialis* (>1.0 to 2.0 cm and >2.0 to 3.0 cm in length); six-category index of estimated percent covers of shell degradation: (1) 0, (2) >0 to 25, (3) >25 to 50, (4) >50 to 75, (5) 75 to <100, and (6) 100 %; NB: no relationships were found in other size-classes of mussels (i.e., ≤1.0, >3.0 to 4.0, and >4.0 cm in length); dashed line = predicted values of the generalised linear model (Table 3); shaded region = standard errors of the prediction.

3.4. Relationship #2: distance from range edge and shell degradation

Shell degradation (an estimate for percent cover of endolithic infestation; *Degradation*) weakly decreased with increasing distance from the warm-edge range limit (*Distance*; Table 2). Moreover, *Distance* only explained about 3 % of the variation in *Degradation* (Table 2). After partitioning the dataset into five size-classes of shell length, the relationship between *Distance* and *Degradation* was found to be significant for the >1.0 to 2.0 and the >2.0 to 3.0 cm size-classes (i.e., intermediate sizes; Fig. 5) but not for the small, ≤1.0 cm, or large, >3.0 to 4.0 and >4.0 cm, size-classes of mussels (Table 3). Despite being a significant predictor, even for the two intermediate size classes, *Distance* only explained about 2 % of variation in *Degradation* (Table 3).

3.5. Relationship #3: shell length and shell degradation

Degradation increased with *Length*, which explained about 41 % of the variation in *Degradation* (Table 2 and Fig. 6). Within sites, the positive relationship between the two was particularly strong at Kidd's Beach (Fig. 6i) and at sites within the range centre between Old Woman's River and Mosselbaai (Fig. 6k–p).

3.6. Relationship #4: distance from range edge and barnacle epibionts

The occurrence of barnacle epibionts on mussel shells (presence-absence *Epibiosis*) increased weakly with distance from the warm-edge range limit (*Distance*), as did the zero-truncated abundance of epibionts (zero-truncated *Epibiosis*; Table 2 and Fig. 7). Overall, *Distance* only explained about 1 % of the variation in the occurrence of epibiosis on shells and <1 % of the variation in the abundance of epibionts (Table 2). After partitioning the dataset into four size-classes of shell lengths, a positive relationship between *Distance* and presence-absence *Epibiosis* was observed

Table 3
Results of partitioned generalised linear models using the Poisson error distribution and the log link function to examine the relationship between distance from warm-edge range limit of the host species, *Mytilus galloprovincialis*, and shell degradation (an estimate for percent cover of endolithic infestation on mussel shells); data partitioned into five size-classes of mussel shell lengths; SE = standard error; statistically significant *p* values are in bold; df = degrees of freedom.

Size-class	Source	Estimate	SE	test statistic (*z*)	*p*
≤1.0 cm	(intercept)	0.46364	0.10345	4.48	**<0.001**
	Distance from range edge	−0.00021	0.00017	−1.24	0.215
	Null deviance	301.94 on 676 df			
	Residual deviance	300.41 on 675 df			
	Deviance explained	<0.01			
>1.0 to 2.0 cm	(intercept)	1.35105	0.03864	34.96	**<0.001**
	Distance from range edge	−0.00033	0.00007	−4.96	**<0.001**
	Null deviance	1,241.3 on 1517 df			
	Residual deviance	1,217.0 on 1516 df			
	Deviance explained	0.02			
>2.0 to 3.0 cm	(intercept)	1.56693	0.02776	56.45	**<0.001**
	Distance from range edge	−0.00014	0.00005	−2.80	**<0.001**
	Null deviance	465.47 on 1,485 df			
	Residual deviance	457.63 on 1,484 df			
	Deviance explained	0.02			
>3.0 to 4.0 cm	(intercept)	1.62516	0.05105	31.84	**<0.001**
	Distance from range edge	−0.00001	0.00009	−0.13	0.899
	Null deviance	58.670 on 380 df			
	Residual deviance	58.654 on 379 df			
	Deviance explained	<0.01			
>4.0 cm	(intercept)	1.66135	0.13812	12.03	**<0.001**
	Distance from range edge	−0.00007	0.00024	−0.28	0.782
	Null deviance	3.4221 on 48 df			
	Residual deviance	3.3458 on 47 df			
	Deviance explained	0.02			

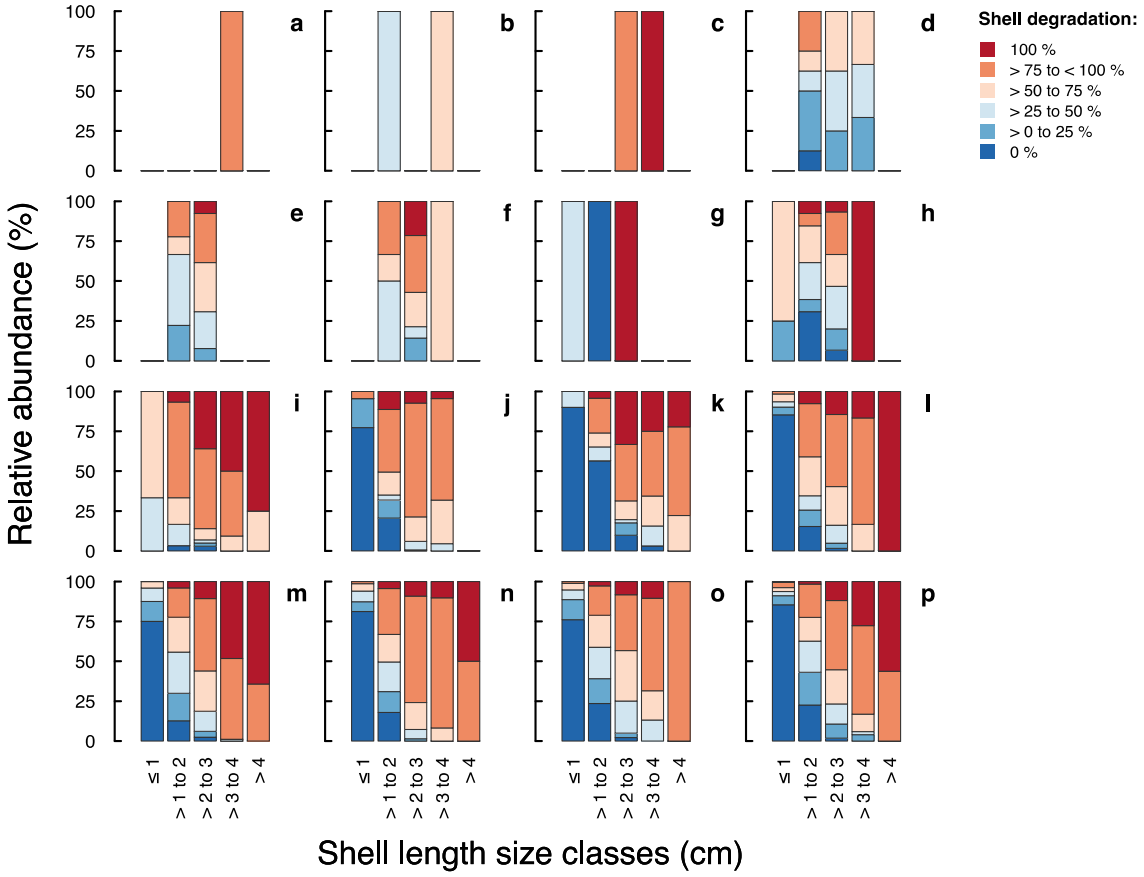

Fig. 6. Relative abundance of different percent covers of shell degradation of *Mytilus galloprovincialis* (also corresponding to the six-category shell degradation index) grouped by shell length size classes from 16 South African sites (ordered from range edge to range centre): (a) Tenza Beach; (b) Mazeppa Bay; (c) Seagulls; (d) Kei Mouth; (e) Morgans Bay; (f) Haga Haga; (g) Cintsa West; (h) Glen Gariff; (i) Kidd's Beach; (j) Hamburg; (k) Old Woman's River; (l) Cannon Rocks; (m) Schoenmakerskop; (n) St Francisbaai; (o) Nature's Valley; (p) Mosselbaai.

for the >1.0 to 2.0 (deviance explained: <1 %), >2.0 to 3.0 (4 %), and >3.0 to 4.0 cm (4 %) size-classes of mussels, but not for the largest size-class (i.e., >4.0 cm; Table 4). For the second component of the models, a negative relationship between *Distance* and zero-truncated *Epibiosis* was detected for the smallest (>1.0 to 2.0 cm; deviance explained: 7 %) and largest (>4.0 cm; 26 %) size-classes of mussels and not for any the intermediate sizes (Table 4).

3.7. Relationship #5: shell length and barnacle epibionts

The occurrence of barnacle epibionts (presence-absence *Epibiosis*), zero-truncated abundance of epibionts on mussel shells (zero-truncated *Epibiosis*), and zero-truncated estimated densities of epibionts on mussel shells (zero-truncated *Epibiosis* after compensating for surface area) all increased with shell length (*Length*; Table 2 and Fig. 7). Moreover, *Length* explained about 18 % of the variation in the occurrence of epibiosis on shells, about 20 % of the variation in the abundance of epibionts, and about 2 % of the variation in estimated densities of epibionts (Table 2). These positive relationships were clearly visible in data for populations from Schoenmakerskop (Fig. 7m) and St Francisbaai (Fig. 7n). At some sites (e.g., Kidd's Beach, Cannon Rocks, Nature's Valley, and Mosselbaai), the occurrence of epibiosis was noticeably low in the largest size-class of mussels (>4.0 cm in shell length). Consequently, we removed shell lengths that were >4.0 cm from the dataset and re-evaluated the relationship between *Length* and *Epibiosis* (abundance and densities) with post hoc two-component conditional models on the subset of data (≤4.0 cm in shell length). Bonferroni correction (alpha level of 0.05 divided by two) was applied, because there were two post hoc tests on the same data. For these post hoc models, the occurrence (presence-absence data), abundance of epibionts (zero-truncated data), and estimated densities of epibionts (zero-truncated data) all increased with increasing *Length* (Table A3 and Fig. A5 in the Appendix), which was consistent with the initial conditional models.

3.8. Relationship #6: shell degradation and barnacle epibionts

Overall, barnacle (*C. dentatus*) epibionts were found on 15.8 % of all mussels that were examined (n = 4,111). Further, only 0.3 % of all examined mussels were endolith-free mussels with barnacle epibionts (n = 11) and 15.5 % were endolith-infested with barnacle epibionts (n = 638). Of the endolith-free mussels, 21.0 % had no barnacle epibionts (n = 863) and 63.2 % were endolith infested with no barnacle epibionts (n = 2,599). Among all the endolith-free mussels (n = 874), few supported epibionts (1.3 %), the majority (98.7 %) being epibiont-free. In comparison, more mussels carried barnacle epibionts among mussels that were endolith infested (i.e., 19.7 % of a total of 3,237 mussels).

Both the occurrence of barnacle epibionts (presence-absence *Epibiosis*) and zero-truncated *Epibiosis* increased with greater shell degradation (*Degradation*; Table 2 and Fig. 8). *Degradation* explained about 13 % of both the variation in the occurrence of epibiosis on shells and the variation in the abundance of epibionts (Table 2). After partitioning the dataset into four size-classes of shell lengths, a positive relationship between *Degradation* and the occurrence of epibionts (presence-absence data) was observed for the >1.0 to 2.0 (deviance explained: 5 %), >2.0 to 3.0 (2 %), and >3.0 to

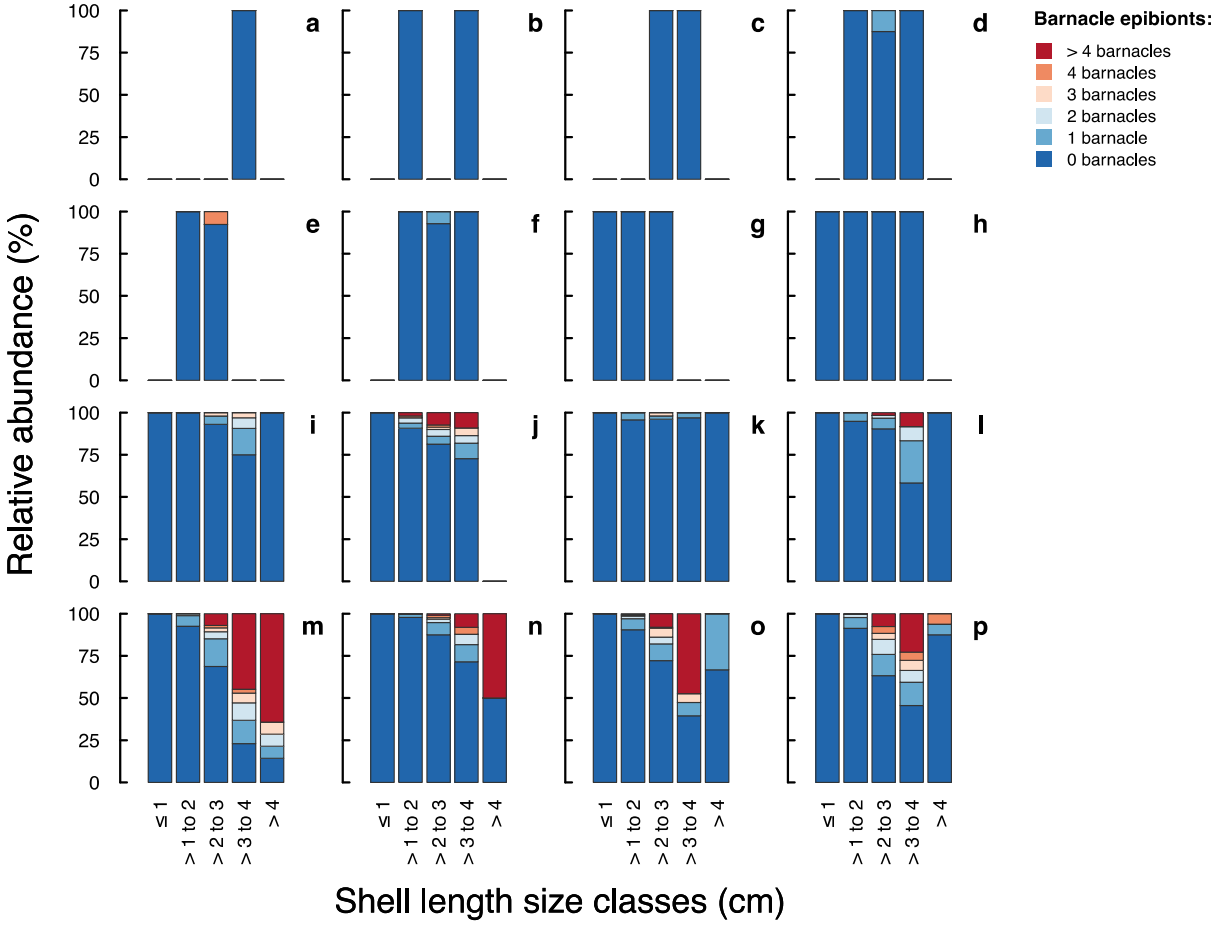

Fig. 7. Relative abundance of different numbers of *Chthamalus dentatus* (barnacle) epibionts on shells of *Mytilus galloprovincialis* grouped by mussel shell length size classes from 16 South African sites. Ordered from range edge to range centre, the sites were: (a) Tenza Beach; (b) Mazeppa Bay; (c) Seagulls; (d) Kei Mouth; (e) Morgans Bay; (f) Haga Haga; (g) Cintsa West; (h) Glen Gariff; (i) Kidd's Beach; (j) Hamburg; (k) Old Woman's River; (l) Cannon Rocks; (m) Schoenmakerskop; (n) St Francisbaai; (o) Nature's Valley; (p) Mosselbaai.

Table 4
Results of partitioned two-component conditional models using the binomial error distribution and the logit link function on presence and absence data for the first component and the Poisson error distribution and the log link function on zero-truncated data for the second component to examine the relationship between distance from warm-edge range limit of the host species, *Mytilus galloprovincialis*, and barnacle epibionts (*Chthamalus dentatus* on mussel shells); data partitioned into four size-classes of mussel shell lengths; NB: no barnacle epibionts were detected on mussel shells ≤1.0 cm in length; SE = standard error; statistically significant *p* values are in bold; df = degrees of freedom.

Size-class	Component	Source	Estimate	SE	test statistic (z)	*p*
>1.0 to 2.0 cm	First	(intercept)	−3.33051	0.32373	−10.29	**<0.001**
		Distance from range edge	0.00125	0.00051	2.47	**0.014**
		Null deviance	763.51 on 1517 df			
		Residual deviance	757.10 on 1516 df			
		Deviance explained	<0.01			
	Second	(intercept)	1.18348	0.20620	5.74	**<0.001**
		Distance from range edge	−0.00107	0.00034	−3.13	**0.002**
		Null deviance	126.48 on 104 df			
		Residual deviance	117.07 on 103 df			
		Deviance explained	0.07			
>2.0 to 3.0 cm	First	(intercept)	−2.32432	0.16787	−13.85	**<0.001**
		Distance from range edge	0.00209	0.00027	7.78	**<0.001**
		Null deviance	1,620.0 on 1,485 df			
		Residual deviance	1,554.5 on 1,484 df			
		Deviance explained	0.04			
	Second	(intercept)	1.32104	0.07969	16.58	**<0.001**
		Distance from range edge	−0.00003	0.00012	−0.24	0.814
		Null deviance	1,301.5 on 348 df			
		Residual deviance	1,301.4 on 347 df			
		Deviance explained	<0.01			
>3.0 to 4.0 cm	First	(intercept)	−1.08587	0.24296	−4.47	**<0.001**
		Distance from range edge	0.00189	0.00043	4.44	**<0.001**
		Null deviance	526.79 on 380 df			
		Residual deviance	506.14 on 379 df			
		Deviance explained	0.04			
	Second	(intercept)	2.11695	0.07360	28.76	**<0.001**
		Distance from range edge	−0.00009	0.00012	−0.75	0.454
		Null deviance	1,649.2 on 178 df			
		Residual deviance	1,648.6 on 177 df			
		Deviance explained	<0.01			
>4.0 cm	First	(intercept)	−0.52282	0.67636	−0.77	0.440
		Distance from range edge	−0.00039	0.00118	−0.33	0.741
		Null deviance	61.906 on 48 df			
		Residual deviance	61.797 on 47 df			
		Deviance explained	<0.01			
	Second	(intercept)	5.05122	0.46620	10.84	**<0.001**
		Distance from range edge	−0.00521	0.00103	−5.05	**<0.001**
		Null deviance	179.11 on 15 df			
		Residual deviance	132.01 on 14 df			
		Deviance explained	0.26			

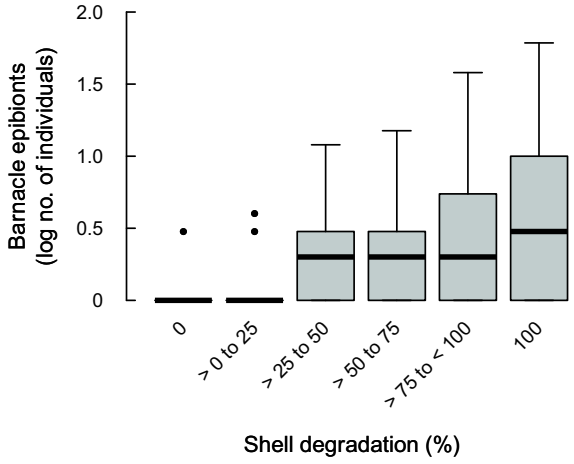

Fig. 8. Zero-truncated abundance of *Chthamalus dentatus* (barnacle) epibionts (log scale) in each of category of estimated percent cover (range: 0 to 100 %) of shell degradation of *Mytilus galloprovincialis* (also corresponding to the six-category shell degradation index); barnacle abundance was $\log_{10}(x)$ transformed.

4.0 cm (3 %) size-classes of mussels, but with no relationship for the largest sizes (i.e., >4.0 cm; Table 5). For the second component of the models, a positive relationship between *Degradation* and the abundance of epibionts (zero-truncated data) was found for each of the four size-classes of mussels (deviance explained ranged from 4 to 10 % depending on the size-class; Table 5).

4. Discussion

The abundance of *Mytilus galloprovincialis* in South Africa is currently centred around the western end of the coastline, including the Namaqua, Southwest Cape and Agulhas bioregions (Ma et al., 2021a; see Fig. 1). This distributional pattern, coupled with seawater temperatures extracted from the literature (i.e., Smit et al., 2013), suggests that EF is acting on the species in the Agulhas bioregion, towards its warm-edge range limit in the east (and probably the case towards its northwestern warm-edge range limit given its slower rates of spread as the species spread towards the Angola–Benguela Front; Branch and Branch, 2018; Ma et al., 2021a). In particular, the abundance of *M. galloprovincialis* exhibits a marked decrease as its range approaches the warmer waters of the Natal bioregion (characterised by a subtropical climate) to the east. During summer, water temperatures tended to be higher at centre sites than range-edge

Table 5
Results of partitioned two-component conditional models using the binomial error distribution and the logit link function on presence and absence data for the first component and the Poisson error distribution and the log link function on zero-truncated data for the second component to examine the relationship between shell degradation (an estimate for percent cover of endolithic infestation on mussel shells) and barnacle epibionts (*Chthamalus dentatus* on mussel shells); data partitioned into four size-classes of mussel shell lengths; NB: no barnacle epibionts were detected on mussel shells ≤1.0 cm in length; SE = standard error; statistically significant *p* values are bolded; df = degrees of freedom.

Size-class	Component	Source	Estimate	SE	test statistic (*z*)	*p*
>1.0 to 2.0 cm	First	(intercept)	−4.20390	0.32090	−13.10	**<0.001**
		Shell degradation	0.43870	0.07500	5.85	**<0.001**
		Null deviance	763.51 on 1,517 df			
		Residual deviance	724.42 on 1,516 df			
		Deviance explained	0.05			
	Second	(intercept)	0.01845	0.25279	0.07	0.942
		Shell degradation	0.12675	0.05551	2.28	**0.022**
		Null deviance	126.48 on 104 df			
		Residual deviance	121.01 on 103 df			
		Deviance explained	0.04			
>2.0 to 3.0 cm	First	(intercept)	−2.54912	0.29562	−8.62	**<0.001**
		Shell degradation	0.29983	0.06209	4.83	**<0.001**
		Null deviance	1,620.0 on 1,485 df			
		Residual deviance	1,594.5 on 1,484 df			
		Deviance explained	0.02			
	Second	(intercept)	−0.22682	0.16748	−1.35	0.176
		Shell degradation	0.31511	0.03316	9.50	**<0.001**
		Null deviance	1,301.5 on 348 df			
		Residual deviance	1,201.5 on 347 df			
		Deviance explained	0.08			
>3.0 to 4.0 cm	First	(intercept)	−2.92320	0.72670	−4.02	**<0.001**
		Shell degradation	0.55210	0.14080	3.92	**<0.001**
		Null deviance	526.79 on 380 df			
		Residual deviance	509.37 on 379 df			
		Deviance explained	0.03			
	Second	(intercept)	0.21733	0.22130	0.98	0.326
		Shell degradation	0.34716	0.04065	8.54	**<0.001**
		Null deviance	1,649.2 on 178 df			
		Residual deviance	1,569.7 on 177 df			
		Deviance explained	0.05			
>4.0 cm	First	(intercept)	−3.33980	2.93000	−1.14	0.254
		Shell degradation	0.47730	0.52850	0.90	0.366
		Null deviance	61.906 on 48 df			
		Residual deviance	61.055 on 47 df			
		Deviance explained	0.01			
	Second	(intercept)	−0.70360	0.84190	−0.84	0.403
		Shell degradation	0.58950	0.14730	4.00	**<0.001**
		Null deviance	179.11 on 15 df			
		Residual deviance	161.99 on 14 df			
		Deviance explained	0.10			

sites, which counter-intuitively indicates that summertime waters approaching the subtropical Natal bioregion were cooler than waters typical of the warm-temperate Agulhas bioregion. Consistent with expectations, however, temperatures were generally lower at centre sites than at range-edge sites in the winter. These seasonal patterns further reveal that seasonal variations in temperature were greater in centre sites than in range-edge sites. Both the seasonal temperatures and seasonality (or lack thereof) likely contribute to the presence and maintenance of EF associated with a thermal stress gradient on *M. galloprovincialis* in the Agulhas bioregion on the south coast of South Africa. Our results suggest that abiotic stress across a thermal gradient (i.e., distance from range edge as our proxy for this gradient) negatively affects densities of *M. galloprovincialis* in mixed-species mussel patches. This gradient in thermal stress also negatively affects densities of the barnacle *Chthamalus dentatus* on emersed rocks; however, its effect on densities of the native mussel, *Perna perna*, in mussel patches is substantially weaker.

To evaluate the importance of the thermal gradient in structuring and maintaining EF across our study area, we gathered evidence from two different sources: interpolated inshore data from the literature and data from loggers installed on intertidal rocks. Effective shore level (ESL) estimations have been developed to delineate periods of emersion and immersion (Harley and Helmuth, 2003; Gilman et al., 2006) and have been widely applied in intertidal ecological studies (e.g., Lathlean et al., 2011; Helmuth et al., 2016; Monaco and McQuaid, 2019; Monaco et al., 2019; Monsinjon et al., 2021). The identification of sudden drops in temperature, revealing the moment when data loggers are immersed in cooler seawater, is sensitive to the temperature threshold that is applied. If the magnitude of the threshold is too low, false positives may be detected (e.g., on a rainy day). As a consequence, this would decrease the reliability of ESL values (Gilman et al., 2006). Conversely, the reliability of ESLs tends to increase with increasing temperature thresholds, but this runs the risk of missing real immersion events during incoming tides and detecting fewer drops. In temperate regions, where estimations of ESL have been predominately applied, temperature thresholds ranging between approximately −4 to −5 °C in 20 min are considered appropriate (and are referred to here as 'conventionally-accepted thresholds'); however, manually lowering the magnitude of the threshold to detect sufficient numbers of sudden drops has been recommended (Gilman et al., 2006). Following this recommendation, we modified the method so that these thresholds could be determined algorithmically for each unique site instead of being subjectively chosen. Our algorithm selected the optimal threshold that detected a sufficient number (≥10) of sudden drops in temperature—while maximising reliability—at our subtropical sites where the conventionally-accepted threshold was too low to detect any drops. In addition, the conventionally accepted method applies a buffer zone of 0.3 m around the mean ESL (Lathlean et al., 2011; Monaco et al., 2019), which potentially discards valid temperature data, especially for sites where the tidal amplitude is low. Our algorithm addressed this problem by using the standard deviation of ESLs to

delineate buffer zones. Overall, our modified method substantially improved how thresholds were algorithmically determined, detecting sufficient numbers of sudden drops for each site and removing uncertain values. In the present study, we were motivated to use immersed in-situ temperatures from our data loggers to compare with interpolated inshore sea temperatures that were extracted from the literature (i.e., Smit et al., 2013). With average differences of 0.9 and 1.2 °C and few outliers, we found there was sufficient agreement between these two sources of data to support the presence of a thermal gradient that is biologically relevant (also see Lathlean et al., 2011).

The abiotic aspect of EF operating through thermal stress may not alone be sufficient to explain most of the variation in species abundance. For example, the combined effects of abiotic conditions and propagule supply explained more of the spatial variation in marine community assemblage across 400 km of shoreline in Chile than EF alone (Valdivia et al., 2015). Physical features of ocean currents and upwelling in South Africa are linked to the regulation of thermal regimes at biogeographic scales, but can also limit larval dispersal (Zardi et al., 2011; Assis et al., 2015). In particular, both the prevailing direction of the Agulhas Current at the species' warm range edge and the upwelling at the cold range edge could transport larvae back towards the range centre and offshore, respectively. Thus, at the species' warm range edge, the Agulhas Current is likely to limit the supply of *M. galloprovincialis* larvae towards the east, lowering recruitment rates to these marginal populations. This is supported by the dearth of small-sized individuals in marginal populations, which suggests that either there is a general scarcity of recruitment for this long-distance dispersing species or newly-recruited individuals experience high levels of mortality (presumably due to EF). In addition, large individuals were also rare in marginal populations, suggesting that the cascading EF-associated effects (i.e., the combined effects of thermal limits, endolithic infestation, and high epibiont loads) may be lethal, resulting in shorter lifespans or slower growth for individuals in range edge sites and longer lifespans and/or faster growth at centre sites. Data from the native range of *M. galloprovincialis* in the Mediterranean Sea show a reduction in filtration rates at temperatures ≥24 °C and an uptick in mortality when temperatures reach ca. 25 °C or higher (Anestis et al., 2010; Gazeau et al., 2014). This is well above the mean summer water temperatures observed from our sites in the warm temperate Agulhas bioregion where the species occurs, but only just above the mean summer water temperatures and below the maximum summer water temperatures from our sites in the subtropical waters of the Natal bioregion where the species is absent. The lethal thermal limit for the species introduced to New Zealand ranges between 35.2 and 37.9 °C, depending on shore height and site (Sorte et al., 2019). Given that *M. galloprovincialis* in southern Africa likely originated from the eastern shores of the Atlantic and not from the Mediterranean Sea (Zardi et al., 2018), sublethal and lethal thermal limits from the Atlantic and southern Africa would be more informative, but are difficult to infer from the literature. For instance, median body temperatures ranging from 16.8 to 17.8 °C might correspond to upper limits of optimal conditions on rocky shores (Monaco and McQuaid, 2018) and maximal heart rate and oxygen consumption observed at ca. 27 °C in water might indicate the onset of sublethal stress (Tagliarolo and McQuaid, 2015; Monaco and McQuaid, 2018). Unlike the native *P. perna*, which exhibits gaping behaviour and evaporative cooling, *M. galloprovincialis* does not gape when exposed to air at low tide (Nicastro et al., 2010, 2012). This makes it more vulnerable to thermal stress despite the effects of endolithic infestation, which increases shell albedo, reducing body temperatures under solar radiation (Nicastro et al., 2012; Zardi et al., 2016; Monsinjon et al., 2021). The combination of higher mortality in marginal populations, lethal and sublethal effects of thermal stress, endolithic infestation, and epibiont load on hosts may dampen the strength of the relationships between the gradient in thermal stress and mussel shell length, shell degradation, and barnacle epibiosis while increasing within-site variability.

The absence of large individuals from marginal populations could also be due to slower growth rates. Growth rates of *M. galloprovincialis* are affected by a range of environmental factors. Growth increases in warmer waters (van Erkom Schurink and Griffiths, 1993), with moderate wave exposure (McQuaid and Lindsay, 2000; Steffani and Branch, 2003), with enhanced small-scale hydrodynamics (McQuaid and Mostert, 2010), and with upwelling (Xavier et al., 2007). Although seasonal growth rates may not vary for some sites, higher growth rates tend to centre around austral summer and autumn seasons for sites where seasonal variation in rates are detectable (Hodgson et al., 2018). From the findings of some of these previous studies, higher growth rates, resulting in larger mussel sizes at a given age, are expected for populations towards the species' range centre where summer temperatures are the highest. Yet no differences in adult shell lengths among sites, excluding the range-edge sites where adults were absent, were found in this study. Although *M. galloprovincialis* settlement varies among sites and years, it does exhibit a conspicuous seasonal peak around austral summer, coincident with elevated seasonal temperatures, though recruitment can extend from spring/early summer to autumn/winter (van Erkom Schurink and Griffiths, 1991; Harris et al., 1998; Bownes and McQuaid, 2009; Pfaff et al., 2011; Reaugh-Flower et al., 2011; Radloff et al., 2021). In the present study, sampling occurred throughout the year, which could have introduced geographic variability in the abundance of small-sized individuals into our dataset. To address this, the relationship was re-assessed after settlers and recruits (i.e., <1.0 cm in length) were removed from the analysis. This revealed a similarly significant relationship between mussel size and distance from its range edge, although only 1–2 % of the variability in mussel size could be explained by distance from range edge, our proxy for EF associated with a thermal stress gradient. This suggests that processes other than EF associated with abiotic gradients (e.g., time since colonisation, biotic interactions with other species) likely play a larger role in controlling growth rates, recruitment, and size-structure in *M. galloprovincialis* populations across its South African range. For example, water flux is believed to be a critical determinant of the population structure of *P. perna* through its influence on the supply of both recruits and food (McQuaid and Lindsay, 2007) and on that of *M. galloprovincialis* because of the effects of wave action on particulate food supply (Bustamante and Branch, 1996).

Again, using distance from the range edge as our proxy for a gradient in thermal stress, EF associated with this gradient was a limited determinant of the amount of shell degradation, our proxy for endolithic infestation, and of barnacle epibiosis. This reflects the substantial variation in shell degradation and barnacle epibiosis within any given site and among different size classes of shells. This also suggests indirect effects of EF on endolithic infestation and epibiosis (i.e., second and third order effects). Post hoc analyses that included size-classes as an additional term in the non-partitioned GzLMs examining Relationships #2, #4, and #6, revealed significant interaction effects for all relationships save Relationship #4 (data not shown). The absence of interaction effects for this post hoc analysis on Relationship #4 (i.e., between barnacle epibiosis and distance from the range edge) suggests that barnacle recruitment on mussel shells of all size-classes was controlled by the same EF-associated gradient as those acting on *M. galloprovincialis* itself. Conversely, there were interaction effects for Relationship #2, between shell degradation and distance from range edge, and for Relationship #6, between barnacle epibiosis and shell degradation. These interactions and the associated partitioned models indicate that size influences both relationships. Firstly, the influence of EF on shell degradation was detectable for mussels of >1.0 to 3.0 cm in length and, secondly, the positive relationship between shell degradation and barnacle epibiosis broke down for individuals >4.0 cm in length. This could be explained by the mortality of two size classes: (a) smaller individuals, driven by increasing effects of EF caused by the thermal gradient towards the range limit (first order effects), and, simultaneously, (b) larger individuals due to higher levels of endolithic infestation and barnacle epibiont load (second and third order EF-associated effects).

Our results revealed that EF associated with a gradient in thermal stress drove cascading effects on shell degradation and barnacle epibiosis on the shells of *M. galloprovincialis*, with implications for the structure of populations located closer to the warm-edge range limit. Our findings suggest that the EF-associated gradient had a direct effect on the abundances of

mussels (*M. galloprovincialis*) and free-living barnacles (*C. dentatus*) across our study area, which was probably due to the cumulative influence of thermal stress on their larval supply, recruitment, post-recruitment survival, and fitness. Conversely, the same EF and thermal gradient acting on *M. galloprovincialis* had a relatively weak effect on the abundance of the co-existing native mussel, *Perna perna*, across our study sites, which all lay within the centre-of-range for that species. Next, we showed that the gradient in thermal stress also had a weak effect on shell degradation, even after controlling for shell size. Yet mussel size was a good determinant for shell degradation. Taken together, we surmise that the changes in population size and size-frequency of shells (i.e., population structure) may have substantially decoupled the influence of EF-associated thermal gradient on shell degradation. Based on first principles, the quality of the periostracum and amount of available space on mussel shells will directly affect the likelihood of barnacle settlement on shells, post-settlement survival of epibiotic barnacles, and their distribution on shells (i.e., settlement on clean vs. damaged areas of the shell). As expected from these first principles, we found that shell degradation was a good determinant of barnacle epibiosis. However, shell degradation was a more limited determinant of barnacle epibiosis when we examined this relationship within different size classes of mussels. Furthermore, the cline in temperature had a relatively weak effect on barnacle epibiosis. This was also the case after controlling for shell size, except for the largest mussels (i.e., >4.0 cm in length) for which the thermal gradient was a good determinant of zero-truncated barnacle abundance. This exception was due to the dearth of large specimens collected from range-edge sites, which was probably caused by lethal EF-associated effects on large mussels and, to a lesser extent, removed by local subsistence harvesters (Rius et al., 2006). The remaining surviving mussels, typically from non-range-edge sites, contributed to the resulting pattern. Taken together, our findings indicate that EF associated with a gradient in temperature has an indirect effect on shell degradation and barnacle epibiosis while, concurrently, shell degradation has a direct effect on barnacle epibiosis. Further intensifying these patterns, the indiscriminate removal of mussels (including *M. galloprovincialis*; Rius et al., 2006) has been carried out by local subsistence harvesters at the range-edge sites and beyond (Siegfried et al., 1985; Hockey and Bosman, 1986; Hockey et al., 1988; Calvo-Ugarteburu et al., 2017). The long-term exploitation of mussels (and other shellfish and macroalgal species) has reduced the complexity of the intertidal rocky shore community (Lasiak, 1991, 1992; Lasiak and Field, 1995), which can adversely affect mussel recruitment into clumps of mussels (as mussels are gregarious) and into tufts of algae (Lasiak and Dye, 1989; Lasiak and Barnard, 1995; Harris et al., 1998; Erlandsson and McQuaid, 2004; Erlandsson et al., 2011). Although it varied from site to site, exploitation intensity tended to be greater towards the range edge and eastwards (i.e., the Transkei region; Rius et al., 2006). Given that our study sites fall within the centre-of-range for *P. perna*, the weak effect of distance on densities of *P. perna* strongly suggests that any effect that could be attributed to the subsistence harvesting, which primarily targeted *P. perna*, was correspondingly limited. Similarly, the effect of subsistence harvesting on densities of *M. galloprovincialis* was probably equally or even more limited, assuming the combined effects of EF associated with a thermal cline and incidental removal of *M. galloprovincialis* during harvesting did not produce any synergistic effects.

5. Conclusions

We record the presence and cascading effects of a thermal stress gradient on the invasive intertidal mussel *M. galloprovincialis* from its range centre to its eastern warm-edge range limit, which is associated with environmental filtering that favours the species in temperate waters but operates against it in subtropical waters. The presence of an EF associated with a gradient in thermal stress in our study area is consistent with in-situ and modelled observations of the species reaching a distributional equilibrium at its eastern limit driven by oceanographic conditions/biogeographic features that limit its eastern spread (McQuaid et al., 2015; Assis et al., 2015; Ma et al., 2021a). The influence of increasing thermal stress on intertidal mussels towards the range edge not only consisted of first order effects, but also second and third order effects of parasitic disease and epibiont load, respectively. This cascade of increasing negative effects with proximity to the species' range edge revealed how an EF-associated abiotic stress gradient can influence the population dynamics of mussels, which can substantially contribute to the maintenance of their distributional limits. Indeed, populations at range edge sites are a product of low settlement rates, high post-settlement mortality, and/or high adult mortality, but probably benefit from the effects of symbiosis/mutualistic breakdown associated with endolithic infestation on mussel shells (Kaehler and McQuaid, 1999; Zardi et al., 2016; Gehman and Harley, 2019; Monsinjon et al., 2021). Emersion temperature may also play an important role in limiting intertidal species (Tagliarolo and McQuaid, 2015; Monaco and McQuaid, 2018; Sorte et al., 2019); however, the present study did not cover a sufficient number of sites (only three within the study region) to determine whether EF associated with a gradient in thermal stress in our study area was also structured and maintained by emersion temperatures, although this seems probable (e.g., Nicastro et al., 2010). In response to global warming in the Anthropocene, mussels are predicted to contract their vertical distribution in the intertidal by shifting their ranges downslope (i.e., narrowing their available habitat), especially at warmer sites (Sorte et al., 2019). Hence, the combined lethal and sublethal effects of emersion and immersion temperatures probably interact to control overall abundance of mussel species as they approach their warm-edge range limits. In addition to abiotic interactions, biotic interactions such as competition, predation, and parasitism can directly and indirectly affect species at their range limits, particularly as biotic interactions are generally more pronounced at their warm range edges than cooler ones (Paquette and Hargreaves, 2021). In our case, however, abiotic effects (a gradient in temperature) appeared to have a stronger influence on mussel population structure than the biotic interactions of endolithic infestation and barnacle epibiosis. The latter (second and third order effects) exhibited relatively weak effects because they were indirectly affected by EF associated with the thermal gradient as a cascade of negative effects.

Significance statement

In the context of range-edge dynamics, this work represents an important contribution to understanding spatial patterns. Recently, biogeographic boundaries or transitions zones have been shown to act as strong or weak barriers to spread of a range-expanding species by reconstructing invasion histories and calculating rate of spread over decadal scales. The present study builds on this work by examining how strong barriers to spread, which is typically associated with suboptimal environmental conditions (i.e., associated with environmental filtering, affect population dynamics towards the range limit. The findings are of general interest because we showed that a gradient in thermal stress is directly affecting population dynamics towards the range edge (first order effect) but also has negative effects, such as increased disease (second order effect) and epibiont load (third order effect).

CRediT authorship contribution statement

Kevin C.K. Ma: Conceptualization, Data curation, Formal analysis, Investigation, Methodology, Visualization, Writing – original draft, Writing – review & editing. **Jonathan R. Monsinjon:** Formal analysis, Software, Writing – review & editing. **P. William Froneman:** Funding acquisition, Resources, Supervision, Writing – review & editing. **Christopher D. McQuaid:** Formal analysis, Funding acquisition, Resources, Supervision, Writing – review & editing.

Data availability

Data and novel code generated from the present study are deposited online in Dryad and available at https://doi.org/10.5061/dryad.h70rxwdmn https://datadryad.org/stash/share/LEfX9e9p_Tb7bu_Ke5wQzAyMVD1uLNLy1OZ-cWl0PX0.

Declaration of competing interest

The authors declare that they have no known competing financial interests or personal relationships that could have appeared to influence the work reported in this paper.

Acknowledgements

We would like to express our thanks to Jaqueline A. Trassierra and Molline N. C. Gusha for their assistance in the field and to Cassandra Barker for providing in situ temperature data. Our thanks also to the South African Navy Hydrographic Office for the 2019 and 2020 hourly tidal predictions. We are indebted to Ticia Swanepoel for administrative support. KCKM conceptualised the study, analyzed the data, and prepared the manuscript with intellectual and editorial input from PWF and CDM. In addition to collecting mussel samples and editorial input, JRM developed the modified method to estimate effective shore level. Collection permits (RES2019/30, RES2020/73) for marine species were issued to the Department of Zoology and Entomology, Rhodes University, by the South African Department of Environmental Affairs, Forestry, and Fisheries (formerly the Department of Agriculture, Forestry, and Fisheries). This project was financially supported by the South African Research Chairs Initiative of the Department of Science and Technology and the National Research Foundation (Grant No. 64801).

Appendix A. Supplementary data

Supplementary data to this article can be found online at https://doi.org/10.1016/j.scitotenv.2022.161184.

References

Anderegg, L.D.L., HilleRisLambers, J., 2019. Local range boundaries vs. large-scale trade-offs: climatic and competitive constraints on tree growth. Ecol. Lett. 22, 787–796. https://doi.org/10.1111/ele.13236.

Anestis, A., Pörtner, H.O., Karagiannis, D., Angelidis, P., Staikou, A., Michaelidis, B., 2010. Response of *Mytilus galloprovincialis* (L.) to increasing seawater temperature and to marteliosis: metabolic and physiological parameters. Comp. Biochem. Physiol. A Mol. Integr. Physiol. 156, 57–66. https://doi.org/10.1016/j.cbpa.2009.12.018.

Assis, J., Zupan, M., Nicastro, K.R., Zardi, G.I., McQuaid, C.D., Serrão, E.A., 2015. Oceanographic conditions limit the spread of a marine invader along Southern Africa shores. PLoS ONE 10, e0128124. https://doi.org/10.1371/journal.pone.0128124.

Bell, C., McQuaid, C.D., Porri, F., 2015. Barnacle settlement on rocky shores: substratum preference and epibiosis on mussels. J. Exp. Mar. Biol. Ecol. 473, 195–201. https://doi.org/10.1016/j.jembe.2015.09.006.

Bers, A.V., Prendergast, G.S., Zürn, C.M., Hansson, L., Head, R.M., Thomason, J.C., 2006. A comparative study of the anti-settlement properties of mytilid shells. Biol. Lett. 2, 88–91. https://doi.org/10.1098/rsbl.2005.0389.

Bownes, S.J., McQuaid, C.D., 2009. Mechanisms of habitat segregation between an invasive and an indigenous mussel: settlement, post-settlement mortality and recruitment. Mar. Biol. 156, 991–1006. https://doi.org/10.1007/s00227-009-1143-z.

Branch, G., Branch, M., 2018. Living Shores: Interacting With Southern Africa's Marine Ecosystems. Struik Nature, Cape Town.

Burnham, K.P., Anderson, D.R., 2002. Model Selection and Multimodel Inference: A Practical Information-Theoretic Approach. second edition. Springer-Verlag, New York.

Buschbaum, C., Saier, B., 2001. Growth of the mussel *Mytilus edulis* L. in the Wadden Sea affected by tidal emergence and barnacle epibionts. J. Sea Res. 45, 27–36. https://doi.org/10.1016/S1385-1101(00)00061-7.

Bustamante, R.H., Branch, G.M., 1996. The dependency of intertidal consumers on kelp-derived organic matter on the west coast of South Africa. J. Exp. Mar. Biol. Ecol. 196, 1–28. https://doi.org/10.1016/0020-0981(95)00093-3.

Calvo-Ugarteburu, G., Raemaekers, S., Halling, C., 2017. Rehabilitating mussel beds in Coffee Bay, South Africa: towards fostering cooperative small-scale fisheries governance and enabling community upliftment. Ambio 46, 214–226. https://doi.org/10.1007/s13280-016-0823-4.

Emanuel, B.P., Bustamante, R.H., Branch, G.M., Eekhout, S., Odendaal, F.J., 1992. A zoogeographic and functional approach to the selection of marine reserves on the west coast of South Africa. S. Afr. J. Mar. Sci. 12, 341–354. https://doi.org/10.2989/02577619209504710.

Enderlein, P., Moorthi, S., Röhrscheidt, H., Wahl, M., 2003. Optimal foraging versus shared doom effects: interactive influence of mussel size and epibiosis on predator preference. J. Exp. Mar. Biol. Ecol. 292, 231–242. https://doi.org/10.1016/S0022-0981(03)00199-0.

Erlandsson, J., McQuaid, C.D., 2004. Spatial structure of recruitment in the mussel *Perna perna* at local scales: effects of adults, algae and recruit size. Mar. Ecol. Prog. Ser. 267, 173–185. https://doi.org/10.3354/meps267173.

Erlandsson, J., McQuaid, C.D., Stanczak, S., 2011. Recruit/algal interaction prevents recovery of overexploited mussel beds: indirect evidence that post-settlement mortality structures mussel populations. Estuar. Coast. Shelf Sci. 92, 132–139. https://doi.org/10.1016/j.ecss.2010.12.028.

Gazeau, F., Alliouane, S., Bock, C., Bramanti, L., López Correa, M., Gentile, M., Hirse, T., Pörtner, H.O., Ziveri, P., 2014. Impact of ocean acidification and warming on the Mediterranean mussel (*Mytilus galloprovincialis*). Front. Mar. Sci. 26, 62. https://doi.org/10.3389/fmars.2014.00062.

Gehman, A.L.M., Harley, C.D.G., 2019. Symbiotic endolithic microbes alter host morphology and reduce host vulnerability to high environmental temperatures. Ecosphere 10, e02683. https://doi.org/10.1002/ecs2.2683.

Gilman, S.E., Harley, C.D.G., Strickland, D.C., Vanderstraeten, O., O'Donnel, M.J., Helmuth, B., 2006. Evaluation of effective shore level as a method of characterising intertidal wave exposure regimes. Limnol. Oceanogr. Methods 4, 448–457. https://doi.org/10.4319/lom.2006.4.448.

Harley, C.D.G., Helmuth, B.S.T., 2003. Local- and regional-scale effects of wave exposure, thermal stress, and absolute versus effective shore level on patterns of intertidal zonation. Limnol. Oceanogr. 48, 1498–1508. https://doi.org/10.4319/lo.2003.48.4.1498.

Harris, J.M., Branch, G.M., Elliott, B.L., Currie, B., Dye, A.H., McQuaid, C.D., Tomalin, B.J., Velasquez, C., 1998. Spatial and temporal variability in recruitment of intertidal mussels around the coast of southern Africa. S. Afr. J. Zool. 33, 1–11. https://doi.org/10.1080/02541858.1998.11448447.

Helmuth, B., Choi, F., Matzelle, A., Torossian, J.L., Morello, S.L., Mislan, K.A.S., Zardi, G., 2016. Long-term, high frequency in situ measurements of intertidal mussel bed temperatures using biomimetic sensors. Sci.Data 3, 160087. https://doi.org/10.1038/sdata.2016.87.

Henry, L.A., Hart, M., 2005. Regeneration and injury and resource allocation in sponges and corals – a review. Int. Rev. Hydrobiol. 90, 125–158. https://doi.org/10.1002/iroh.200410759.

Hockey, P.A.R., Bosman, A.L., 1986. Man as an intertidal predator in Transkei: disturbance, community convergence and management of a natural food resource. Oikos 46, 3–14. https://doi.org/10.2307/3565373.

Hockey, P.A.R., Bosman, A.L., Siegfried, W.R., 1988. Patterns and correlates of shellfish exploitation by coastal people in Transkei: an enigma of protein production. J. Appl. Ecol. 25, 353–363. https://doi.org/10.2307/2403631.

Hodgson, A.N., Claassens, L., Kankondi, S., 2018. Shell morphometrics and growth rate of the invasive bivalve mollusc *Mytilus galloprovincialis* in the Knysna estuarine embayment, South Africa. Afr. J. Aquat. Sci. 43, 367–374. https://doi.org/10.2989/16085914.2018.1539647.

Kaehler, S., 1999. Incidence and distribution of phototrophic shell-degrading endoliths of the brown mussel *Perna perna*. Mar. Biol. 135, 505–514. https://doi.org/10.1007/s002270050651.

Kaehler, S., McQuaid, C.D., 1999. Lethal and sub-lethal effects of phototrophic endoliths attacking the shell of the intertidal mussel *Perna perna*. Mar. Biol. 135, 497–503. https://doi.org/10.1007/s002270050650.

Kampfer, A., 2017. South african tide tables 2019. South African Navy, Tokai, Cape Town.

Kampfer, A., 2018. South African Tide Tables 2020. South African Navy, Tokai, Cape Town.

Kraft, N.J.B., Adler, P.B., Godoy, O., James, E.C., Fuller, S., Levine, J.M., 2015. Community assembly, coexistence and the environmental filtering metaphor. Funct. Ecol. 29, 592–599. https://doi.org/10.1111/1365-2435.12345.

Lasiak, T., 1991. The susceptibility and/or resilience of rocky littoral molluscs to stock depletion by the indigenous coastal people of Transkei, southern Africa. Biol. Conserv. 56, 245–264. https://doi.org/10.1016/0006-3207(91)90060-M.

Lasiak, T., 1992. Contemporary shellfish-gathering practices of indigenous coastal people in Transkei: some implications for interpretation of the archaeological record. S. Afr. J. Sci. 88, 19–28 10520/AJA00382353_9423.

Lasiak, T.A., Barnard, T.C.E., 1995. Recruitment of the brown mussel *Perna perna* onto natural substrata: a refutation of the primary/secondary settlement hypothesis. Mar. Ecol. Prog. Ser. 120, 147–153. https://doi.org/10.3354/meps120147.

Lasiak, T., Dye, A., 1989. The ecology of the brown mussel *Perna perna* in Transkei, Southern Africa: implications for the management of a traditional food resource. Biol. Conserv. 47, 245–257. https://doi.org/10.1016/0006-3207(89)90068-2.

Lasiak, T.A., Field, J.G., 1995. Community-level attributes of exploited and non-exploited rocky infratidal macrofaunal assemblages in Transkei. J. Exp. Mar. Biol. Ecol. 185, 33–53. https://doi.org/10.1016/0022-0981(94)00130-6.

Lathlean, J.A., Ayre, D.J., Minchinton, T.E., 2011. Rocky intertidal temperature variability along the southeast coast of Australia: comparing data from in situ loggers, satellite-derived SST and terrestrial weather stations. Mar. Ecol. Prog. Ser. 439, 83–95. https://doi.org/10.3354/meps09317.

Laudien, J., Wahl, M., 1999. Indirect effects of epibiosis on host mortality: seastar predation on differently fouled mussels. Mar. Ecol. 20, 35–47. https://doi.org/10.1046/j.1439-0485.1999.00063.x.

Laudien, J., Wahl, M., 2004. Associational resistance of fouled blue mussels (*Mytilus edulis*) against starfish (*Asterias rubens*) predation: relative importance of structural and chemical properties of the epibionts. Helgol. Mar. Res. 58, 162–167. https://doi.org/10.1007/s10152-004-0181-7.

Ma, K.C.K., McQuaid, C.D., Pulfrich, A., Robinson, T.B., 2020. Status of a decennial marine invasion by the bisexual mussel *Semimytilus algosus* (Gould, 1850) in South Africa. Afr. J. Mar. Sci. 42, 507–515. https://doi.org/10.2989/1814232X.2020.1820376xa.

Ma, K.C.K., Gusha, M.N.C., Zardi, G.I., Nicastro, K.R., Monsinjon, J.R., McQuaid, C.D., 2021a. Biogeographic drivers of distribution and abundance in an alien ecosystem engineer: transboundary range expansion, barriers to spread, and spatial structure. J. Biogeogr. 48, 1941–1959. https://doi.org/10.1111/jbi.14124.

Ma, K.C.K., Redelinghuys, S., Gusha, M.N.C., Dyantyi, S.B., McQuaid, C.D., Porri, F., 2021b. Intertidal estimates of sea urchin abundance reveal congruence in spatial structure for a guild of consumers. Ecol.Evol. 11, 11930–11944. https://doi.org/10.1002/ece3.7958.

Marquet, N., Nicastro, K.R., Gektidis, M., McQuaid, C.D., Pearson, G.A., Serrão, E.A., Zardi, G.I., 2013. Comparison of photographic shell-degrading endoliths in invasive and native populations of the intertidal mussel *Mytilus galloprovincialis*. Biol. Invasions 15, 1253–1272. https://doi.org/10.1007/s10530-012-0363-1.

McQuaid, C.D., Lindsay, T.L., 2000. The effects of wave exposure on growth and mortality rates of the mussel *Perna perna*: bottom-up regulation of intertidal populations. Mar. Ecol. Prog. Ser. 206, 147–154. https://doi.org/10.3354/meps206147.

McQuaid, C.D., Lindsay, T.L., 2007. Wave exposure effects on population structure and recruitment in the mussel *Perna perna* suggest regulation primarily through availability of recruits and food, not space. Mar. Biol. 151, 2123–2131. https://doi.org/10.1007/s00227-007-0645-9.

McQuaid, C.D., Mostert, B.P., 2010. The effects of within-shore water movement on growth of the intertidal mussel *Perna perna*: an experimental field test of bottom-up control at centimetre scales. J. Exp. Mar. Biol. Ecol. 384, 119–123. https://doi.org/10.1016/j.jembe.2010.01.005.

McQuaid, C.D., Porri, F., Nicastro, K.R., Zardi, G.I., 2015. Simple, scale-dependent patterns emerge from very complex effects–an example from the intertidal mussels *Mytilus galloprovincialis* and *Perna perna*. Oceanogr. Mar. Biol. Annu. Rev. 53, 127–156.

Monaco, C.J., McQuaid, C.D., 2018. Applicability of dynamic energy budget (DEB) models across steep environmental gradients. Sci. Rep. 8, 16384. https://doi.org/10.1038/s41598-018-34786-w.

Monaco, C.J., McQuaid, C.D., 2019. Climate warming reduces the reproductive advantage of a globally invasive intertidal mussel. Biol. Invasions 21, 2503–2516. https://doi.org/10.1007/s10530-019-01990-2.

Monaco, C.J., Porporato, E.M.D., Lathlean, J.A., Tagliarolo, M., Sarà, G., McQuaid, C.D., 2019. Predicting the performance of cosmopolitan species: dynamic energy budget model skill drops across large spatial scales. Mar. Biol. 166, 14. https://doi.org/10.1007/s00227-018-3462-4.

Monsinjon, J.R., McQuaid, C.D., Nicastro, K.R., Seuront, L., Oróstica, M.H., Zardi, G.I., 2021. Weather and topography regulate the benefit of a conditionally helpful parasite. Funct. Ecol. 35, 2691–2706. https://doi.org/10.1111/1365-2435.13939.

Ndhlovu, A., McQuaid, C.D., Nicastro, K., Marquet, N., Gektidis, M., Monaco, C.J., Zardi, G., 2019. Biogeographic patterns of endolithic infestation in an invasive and an indigenous intertidal marine ecosystem engineer. Diversity 11, 75. https://doi.org/10.3390/d11050075.

Ndhlovu, A., McQuaid, C.D., Monaco, C.J., 2021. Ectoparasites reduce scope for growth in a rocky-shore mussel (*Perna perna*) by raising maintenance costs. Sci. Total Environ. 753, 142020. https://doi.org/10.1016/j.scitotenv.2020.142020.

Nicastro, K.R., Zardi, G.I., McQuaid, C.D., Stephens, L., Radloff, S., Blatch, L., 2010. The role of gaping behaviour in habitat partitioning between coexisting intertidal mussels. BMC Ecol. 10, 17. https://doi.org/10.1186/1472-6785-10-17.

Nicastro, K.R., Zardi, G.I., McQuaid, C.D., Pearson, G.A., Serrão, E.A., 2012. Love thy neighbour: group properties of gaping behaviour in mussel aggregations. PLoS ONE 7, e47382. https://doi.org/10.1371/journal.pone.0047382.

Oldfather, M.F., Kling, M.M., Sheth, S.N., Emery, N.C., Ackerly, D.D., 2020. Range edges in heterogeneous landscapes: integrating geographic scale and climate complexity into range dynamics. Glob. Chang. Biol. 26, 1055–1067. https://doi.org/10.1111/gcb.14897.

Paine, C.E.T., Norden, N., Chave, J., Forget, P.M., Fortunel, C., Dexter, K.G., Baraloto, C., 2012. Phylogenetic density dependence and environmental filtering predict seedling mortality in a tropical forest. Ecol. Lett. 15, 34–41. https://doi.org/10.1111/j.1461-0248.2011.01705.x.

Paquette, A., Hargreaves, A.L., 2021. Biotic interactions are more often important at species'warm versus cool range edges. Ecol. Lett. 24, 2427–2438. https://doi.org/10.1111/ele.13864.

Pfaff, M.C., Branch, G.M., Weiters, E.A., Branch, R.A., Broitman, B.R., 2011. Upwelling intensity and wave exposure determine recruitment of intertidal mussels and barnacles in the southern Benguela upwelling region. Mar. Ecol. Prog. Ser. 425, 141–152. https://doi.org/10.3354/meps09003.

Puccinelli, E., McQuaid, C.D., 2021. Commensalism, antagonism or mutualism? Effects of epibiosis on the trophic relationships of mussels and epibiotic barnacles. J. Exp. Mar. Biol. Ecol. 540, 151549. https://doi.org/10.1016/j.jembe.2021.151549.

R Core Team, 2020. R: a language and environment for statistical computing. R Foundation for Statistical Computing, Vienna, Austria. http://www.r-project.org/.

Radloff, J., Hodgson, A.N., Claasens, L., 2021. Settlement of the invasive mussel *Mytilus galloprovincialis* in a warm temperate estuarine embayment in South Africa. Afr. J. Aquat. Sci. 46, 206–214. https://doi.org/10.2989/16085914.2020.1842170.

Reaugh-Flower, K., Branch, G.M., Harris, J.M., McQuaid, C.D., Currie, B., Dye, A., Robertson, B., 2011. Scale-dependent patterns and processes of intertidal mussel recruitment around southern Africa. Mar. Ecol. Prog. Ser. 434, 101–119. https://doi.org/10.3354/meps09169.

Rius, M., Kaehler, S., McQuaid, C.D., 2006. The relationship between human exploitation pressure and condition of mussel populations along the south coast of South Africa. S. Afr. J. Sci. 102, 130–136 10520/EJC96520.

Rohatgi, A., 2020. WebPlotDigitizer, Version 4.4. Pacifica, California, USA. https://automeris.io/WebPlotDigitizer.

Sagarin, R.D., Gaines, S.D., 2002. Geographical abundance distributions of coastal invertebrates: using one-dimensional ranges to test biogeographic hypotheses. J. Biogeogr. 29, 985–997. https://doi.org/10.1046/j.1365-2699.2002.00705.x.

Scardino, A., de Nys, R., 2004. Fouling deterrence on the bivalve shell *Mytilus galloprovincialis*: a physical phenomenon? Biofouling 20, 249–257. https://doi.org/10.1080/08927010400016608.

Scardino, A., de Nys, R., Ison, O., O'Connor, W., Steinberg, P., 2003. Microtopography and antifouling properties of the shell surface of the bivalve molluscs *Mytilus galloprovincialis* and *Pinctada imbricata*. Biofouling 19, 221–230. https://doi.org/10.1080/0892701021000057882.

Siegfried, W.R., Hockey, P.A.R., Crowe, A.A., 1985. Exploitation and conservation of brown mussel stocks by coastal people of Transkei. Environ. Conserv. 12, 303–307. https://doi.org/10.1017/S037689290003441X.

Smit, A.J., Roberts, M., Anderson, R.J., Dufois, F., Dudley, S.F.J., Bornman, T.G., Olbers, J., Bolton, J.J., 2013. A coastal seawater temperature dataset for biogeographical studies: large biases between in situ and remotely-sensed data sets arounds the coast of South Africa. PLoS ONE 8, e81944. https://doi.org/10.1371/journal.pone.0081944.

Sommer, B., Harrison, P.L., Beger, M., Pandolfi, J.M., 2014. Trait-mediated environmental filtering drives assembly at biogeographic transition zones. Ecology 95, 1000–1009. https://doi.org/10.1890/13-1445.1.

Sorte, C.J.B., Bernatchez, G., Mislan, K.A.S., Pandori, L.L.M., Sibiger, N.H., Wallingford, P.D., 2019. Thermal tolerance limits as indicators of current and future intertidal zonation patterns in a diverse mussel guild. Mar. Biol. 166, 6. https://doi.org/10.1007/s00227-018-3452-6.

Steffani, C.N., Branch, G.M., 2003. Growth rate, condition, and shell shape of *Mytilus galloprovincialis*: responses to wave exposure. Mar. Ecol. Prog. Ser. 246, 197–209. https://doi.org/10.3354/meps246197.

Stephenson, T.A., Stephenson, A., 1949. The universal features of zonation between tidemarks on rocky coasts. J. Ecol. 37, 289–305. https://doi.org/10.2307/2256610.

Tagliarolo, M., McQuaid, C.D., 2015. Sub-lethal and sub-specific temperature effects are better predictors of mussel distribution than thermal tolerance. Mar. Ecol. Prog. Ser. 535, 145–159. https://doi.org/10.3354/meps11434.

Thieltges, D.W., Buschbaum, C., 2007a. Mechanism of an epibiont burden: *Crepidula fornicata* increases byssus thread production by *Mytilus edulis*. J. Molluscan Stud. 73, 75–77. https://doi.org/10.1093/mollus/eyl033.

Thieltges, D.W., Buschbaum, C., 2007b. Vicious circle in the intertidal: facilitation between barnacle epibionts, a shell boring polychaete and trematode parasites in the periwinkle *Littorina littorea*. J. Exp. Mar. Biol. Ecol. 340, 90–95. https://doi.org/10.1016/j.jembe.2006.08.014.

Valdivia, N., Aguilera, M.A., Navarrete, S.A., Broitman, B.R., 2015. Disentangling the effects of propagule supply and environmental filtering on the spatial structure of a rocky shore metacommunity. Mar. Ecol. Prog. Ser. 538, 67–79. https://doi.org/10.3354/meps11493.

van Erkom Schurink, C., Griffiths, C.L., 1991. A comparison of reproductive cycles and reproductive output in four Southern African mussel species. Mar. Ecol. Prog. Ser. 76, 123–134. https://doi.org/10.3354/meps076123.

van Erkom Schurink, C., Griffiths, C.L., 1993. Factors affecting relative rates of growth in four South African mussel species. Aquaculture 109, 257–273. https://doi.org/10.1016/0044-8486(93)90168-X.

Wahl, M., 2008. Ecological lever and interface ecology: epibiosis modulates the interactions between host and environment. Biofouling 24, 427–438. https://doi.org/10.1080/08927010802339772.

Xavier, B.M., Branch, G.M., Wieters, E., 2007. Abundance, growth and recruitment of *Mytilus galloprovincialis* on the west coast of South Africa in relation to upwelling. Mar. Ecol. Prog. Ser. 346, 189–201. https://doi.org/10.3354/meps07007.

Zardi, G.I., McQuaid, C.D., Teske, P.R., Barker, N.P., 2007. Unexpected genetic structure of mussel populations in South Africa: indigenous *Perna perna* and invasive *Mytilus galloprovincialis*. Mar. Ecol. Prog. Ser. 337, 135–144. https://doi.org/10.3354/meps337135.

Zardi, G.I., Nicastro, K.R., McQuaid, C.D., Gektidis, M., 2009. Effects of endolithic parasitism on invasive and indigenous mussels in a variable physical environment. PLoS ONE 4, e6560. https://doi.org/10.1371/journal.pone.0006560.

Zardi, G.I., Nicastro, K.R., McQuaid, C.D., Hancke, L., Helmuth, B., 2011. The combination of selection and dispersal helps explain genetic structure in intertidal mussels. Oecologia 165, 947–958. https://doi.org/10.1007/s00442-010-1788-9.

Zardi, G.I., Nicastro, K.R., McQuaid, C.D., Ng, T.P.T., Lathlean, J., Seuront, L., 2016. Enemies with benefits: parasitic endoliths protect mussels against heat stress. Sci. Rep. 6, 31413. https://doi.org/10.1038/srep31413.

Zardi, G.I., McQuaid, C.D., Jacinto, R., Lourenço, C.R., Serrão, E.A., Nicastro, K.R., 2018. Reassessing the origins of the invasive mussel *Mytilus galloprovincialis* in southern Africa. Mar. Freshw. Res. 69, 607–613. https://doi.org/10.1071/MF17132.

Zuykov, M., Anderson, J., Kolyuchkina, G., Zhao, L., Shirai, K., Gosselin, M., Archambault, P., Schindler, M., 2021. New three-way symbiosis: an eukaryotic alga, a blue mussel, and endolithic cyanobacteria. Symbiosis 84, 163–169. https://doi.org/10.1007/s13199-021-00777-1.